

Manifold Principle Component Analysis for Large-Dimensional Matrix Elliptical Factor Model

ZeYu Li ^{*,§}, Yong He [‡], Xinbing Kong ^{‡,§}, Xinsheng Zhang ^{*}

March 29, 2022

Abstract

Matrix factor model has been growing popular in scientific fields such as econometrics, which serves as a two-way dimension reduction tool for matrix sequences. In this article, we for the first time propose the matrix elliptical factor model, which can better depict the possible heavy-tailed property of matrix-valued data especially in finance. Manifold Principle Component Analysis (MPCA) is for the first time introduced to estimate the row/column loading spaces. MPCA first performs Singular Value Decomposition (SVD) for each “local” matrix observation and then averages the local estimated spaces across all observations, while the existing ones such as 2-dimensional PCA first integrates data across observations and then does eigenvalue decomposition of the sample covariance matrices. We propose two versions of MPCA algorithms to estimate the factor loading matrices robustly, without any moment constraints on the factors and the idiosyncratic errors. Theoretical convergence rates of the corresponding estimators of the factor loading matrices, factor score matrices and common components matrices are derived under mild conditions. We also propose robust estimators of the row/column factor numbers based on the eigenvalue-ratio idea, which are proven to be consistent. Numerical studies and real example on financial returns data check the flexibility of our model and the validity of our MPCA methods.

Keywords: Factor Model; Grassmann manifold; Matrix elliptical distribution; Principle component analysis.

1 Introduction

Factor models have been a classical dimension reduction tool in statistics, which is popular for its ability to summarize information in large data sets. More importantly, factor models characterize many economic problems, e.g., the Arbitrage Pricing Theory of [Ross \(1976\)](#). In the last two decades large-dimensional approximate factor model is growing popular as we embrace the big data era where more and more variables are recorded and stored, see the seminal work by [Bai and Ng \(2002\)](#) and [Stock and Watson \(2002\)](#), and some representative work by [Bai \(2003\)](#), [Onatski \(2009\)](#), [Ahn and Horenstein](#)

^{*}Department of Statistics, School of Management at Fudan University, China; e-mail:zeyuli21@m.fudan.edu.cn; xszhang@fudan.edu.cn

[†]Institute of Financial Studies, Shandong University, China; e-mail:heyong@sdu.edu.cn

[‡]Nanjing Audit University, China; e-mail:xinbingkong@126.com

[§]The authors contributed equally to this work.

(2013), Fan et al. (2013), Bai and Li (2012), Bai and Li (2016) and Trapani (2018). The aforementioned papers all require the fourth moments (or even higher moments) of factors and idiosyncratic errors exist, which may be constrictive in research areas such as finance. He et al. (2022) for the first time propose a Robust Two Step (RTS) procedure to do factor analysis without any moment constraints, under the framework of elliptical distributions, see also the endeavors by Yu et al. (2019), He et al. (2020) and Chen et al. (2021a).

The modern data collected are usually well-structured in a matrix form, such as time list of tables recording several macroeconomic variables across a number of countries; a series of customers' ratings on a large number of items in an online platform, see Chen and Fan (2021) for further examples of well-structured matrix observations. In the last few years, matrix factor model has drawn growing attention as an important two-way dimension reduction tool for matrix sequences. Wang et al. (2019) for the first time proposed the following matrix factor model:

$$\underbrace{X_t}_{p \times q} = \underbrace{R}_{p \times p_0} \times \underbrace{F_t}_{p_0 \times q_0} \times \underbrace{C^T}_{q_0 \times q} + \underbrace{E_t}_{p \times q}, \quad (1.1)$$

where $\{X_t, 1 \leq t \leq T\}$ are matrix observations of dimension $p \times q$, R is the row factor loading matrix exploiting the variations of X_t across the rows, C is the $q \times q_0$ column factor loading matrix reflecting the differences across the columns of X_t , F_t is the common factor matrix for all cells in X_t and E_t is the idiosyncratic components. A naive way to do factor analysis for matrix observations is to first vectorize the data X_t , and then to adopt the classical well-developed vector factor models techniques. However, when data genuinely have a matrix factor structure as in (1.1), this naive approach would lead to sub-optimal inference (Chen and Fan, 2021; He et al., 2021c). Two different types of matrix factor model assumptions are adopted in the existing literature. One type of models assumes that the factors accommodate all dynamics, making the idiosyncratic noise “white” with no autocorrelation but allowing substantial contemporary cross-correlation among the error process, and the estimation of the loading space is done by an eigen-analysis of the nonzero lag autocovariance matrices, see for example Wang et al. (2019). The other type of models assumes that a common factor must have impact on almost all (defined asymptotically) of the matrix time series, but allows the idiosyncratic noise to have weak cross-correlations and weak autocorrelations, and principle component analysis (PCA) of the sample covariance matrix is typically used to estimate the spaces spanned by the row/column loading matrices, see for example Chen and Fan (2021); Yu et al. (2021); He et al. (2021a). As far as we know, all the existing work on matrix factor model assumes that the fourth moments (or even higher moments) of factors and idiosyncratic errors exist, which could be restrictive in real applications such as in finance. Figure 1 depicts the boxplots of the row factor loading estimation errors based on 100 replications, from which we can see that the $(2D)^2$ -PCA by Zhang and Zhou (2005) and the Projection Estimation (PE) method by Yu et al. (2021) results in bigger biases and higher dispersions as the distribution tails become heavier.

In the current work, we for the first time propose a freshly new and flexible model, named as the Matrix Elliptical Factor Model (MEFM), which assumes that the factor matrix F_t and the idiosyncratic errors matrix E_t follow an joint Elliptical Matrix Distribution (EMD), which covers a large class of heavy-tailed matrix distributions such as matrix t -distribution. To estimate the row (column) loading

space $\text{Span}(R)$ ($\text{Span}(C)$) of MEFM robustly, we propose a Manifold Principle Component Analysis (MPCA) method for the first time. In essence, for each data matrix X_t , assume that $p_0 = q_0 = r_0$ for better illustration, the MPCA first finds the best r_0 -dimensional row (column) loading space estimator $\text{Span}(\hat{R}_t)$ ($\text{Span}(\hat{C}_t)$), which can be viewed as an element in the Grassmann manifold $\mathcal{G}(p_0, p)$ ($\mathcal{G}(q_0, q)$), where the Grassmann manifold $\mathcal{G}(p_0, p)$ is the set of p_0 -dimensional linear subspaces of the \mathbb{R}^p (Ham and Lee, 2008). Then MPCA looks for the “centers” of all row/column loading space estimators within their Grassmann manifolds respectively. According to the way of finding the best linear row/column space for each matrix observation, the MPCA then has two versions, MPCA_{op} and MPCA_F , corresponding to the optimization problem (2.2) under matrix operator norm and matrix Frobenius norm respectively. For the MPCA_F , the projection technique in Yu et al. (2021) happens to be taken into account, which increases the signal-to-noise ratio. Now, let us come back to Figure 1, in which we also presented the results using the MPCA_{op} and MPCA_F methods. It can be seen that MPCA_F always performs well under various distributions, and is even not sensitive to the elliptical assumption (noting that α -stable distribution is not elliptical). The MPCA_{op} method also exhibits an extent of robustness, while it is inferior to the MPCA_F in all cases. This indicates that for matrix factor model, the projection technique is always preferred as it can increase the signal-to-noise ratio.

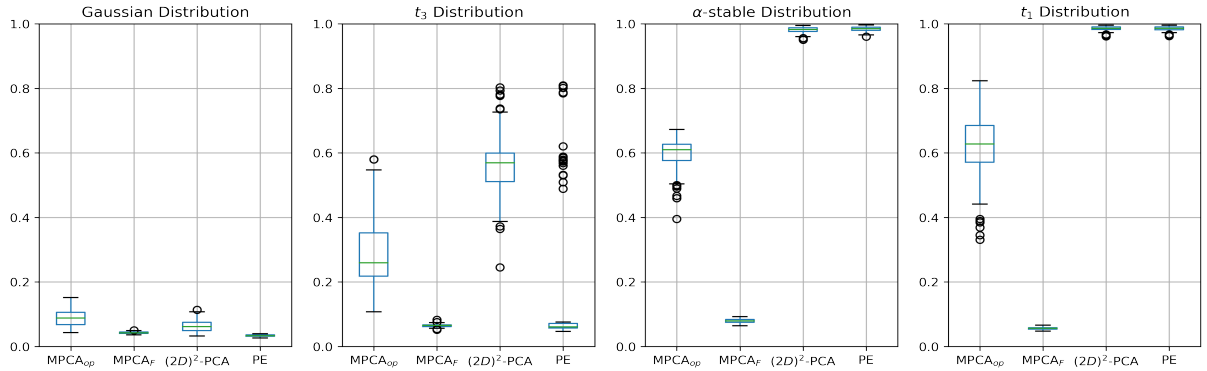


Figure 1: Boxplot of the distance between the estimated row loading space \hat{R} and the true row loading space R by MPCA_{op} , MPCA_F , $(2D)^2$ -PCA and PE methods under different distributions (normal, t_3 , α -stable with $\alpha = 1.8$ and t_1), $p = q = 100$, $T = 300$. The noises are scaled to get comparable performance under various distributions.

To do matrix factor analysis, the first step is to determine the pair of factor numbers. As for the Elliptical Matrix Factor Model (MFM), both the row and column factor numbers should be predetermined. Wang et al. (2019) proposed to estimate the pair of factor numbers by the ratios of consecutive eigenvalues of auto-covariance matrices; Chen and Fan (2021) proposed an α -PCA based eigenvalue-ratio method and Yu et al. (2021) further proposed a projection-based iterative eigenvalue-ratio method, all borrowing the eigenvalue ratio idea from Ahn and Horenstein (2013). He et al. (2021a) is the only work that determines the pair of factor numbers from the perspective of sequential hypothesis testing. In this article we also propose similar eigenvalue ratio methods based on the MPCA approach. The proposed estimators of the pair of factor numbers are proven to be consistent under mild conditions and performs much better than the existing ones when the matrix-valued data are heavy-tailed shown in the simulation study.

The contributions of the current work lie in the following aspects. Firstly, we for the first time propose a flexible matrix elliptical factor model for matrix observations which is adaptive to their tail properties. Secondly, to estimate the loading spaces of MEFM robustly, we for the first time introduce a freshly new principle component analysis method, named as the Manifold Principle Component Analysis (MPCA), which is computationally efficient and easy to implement. The MPCA is completely different from the traditional PCAs (e.g., the α -PCA by [Chen and Fan \(2021\)](#) and $(2D)^2$ -PCA by [Zhang and Zhou \(2005\)](#)) method in the sense that MPCA first performs Singular Value Decomposition (SVD) for each “local” matrix observation and then integrates/averages the local spaces, while the traditional PCAs first integrates the matrix observations and then finds the principle eigenvectors of the sample covariance matrices. Clearly, the MPCA would show great computational advantage especially in online updating problems. Thirdly, the theoretical guarantee of MPCA relies heavily on the properties of the expected projection matrices, which has not aroused much attention in existing literatures. We show that the expected projection matrices contain adequate subspace information, which is of independent interest. At last, the theoretical analysis shows that the proposed MPCA estimators are consistent without any moment constraints on the underlying distributions of the factors and the idiosyncratic errors, which generalize the methods’ applicability to heavy-tailed datasets such as financial returns.

The remainder of the article is organized as follows. In Section 2, we first introduce the proposed matrix elliptical factor model. Then we introduce the Manifold Principle Component Analysis (MPCA) method, and take the special degenerated case $q = 1$ to illustrate the intuition of its robustness. At last we introduce the best subspace approximation for each matrix observation X_t under both the matrix operator norm and the matrix Frobenius norm, by which we further propose the two versions of MPCA algorithms. In Section 3, we investigate the theoretical properties of the estimators by MPCA, including the factor loadings, factor scores and common components matrices. In Section 4, we further discuss the selection of the pair of factor numbers and propose two procedures based on the eigenvalue ratio idea. In section 5, we conduct thorough numerical studies to illustrate the advantages/robustness of the MPCA method and the corresponding eigenvalue-ratio factor number estimation methods over the state-of-the-art methods. In Section 6, we analyze a financial returns dataset to illustrate the practical value of the proposed methods. We conclude the article and discuss the limitation of the current work and possible future research directions in Section 7. The proofs of the main theorems and additional details are collected in the supplementary materials.

To end this section, we introduce some notations throughout the study. For matrix A , $\|A\|_{op}$ and $\|A\|_F$ represent the operator norm and Frobenius norm, $\text{tr}(A)$ denotes the trace of A , and $\text{Vec}(A)$ means vectorization, $\sigma_i(A)$ denotes the i -th largest singular value of A . Moreover, if A is symmetric, $\lambda_i(A)$ denotes the i -th largest eigenvalue of A , and let $d_i(A) = (\lambda_i - \lambda_{i+1})(A)$ be the i -th eigengap. For vector a , denote l^2 -norm as $\|a\|_2$. The notation $\stackrel{d}{=}$ means identically distributed. The o_p is for convergence to zero in probability and O_p is for stochastic boundedness. For two random series X_n and Y_n , $X_n \lesssim Y_n$ means that $X_n = O_p(Y_n)$, and $X_n \gtrsim Y_n$ means that $Y_n = O_p(X_n)$. The notation $X_n \asymp Y_n$ means that $X_n \lesssim Y_n$ and $X_n \gtrsim Y_n$. $\mathcal{O}_{p,q}$ denotes the space of $p \times q$ matrices with orthogonal columns. $[x]$ means rounding x to the nearest integer. The constants c and C may not be identical in different lines.

2 Methodology

2.1 Matrix Elliptical Factor Model

For $p \times q$ matrix-variate sequences $\{X_t, t = 1, \dots, T\}$, the centered matrix factor model is introduced by Wang et al. (2019) as follows:

$$X_t = RF_tC^\top + E_t, \quad t = 1, \dots, T,$$

where R is the $p \times p_0$ row factor loading matrix, C is the $q \times q_0$ column factor loading matrix, F_t is the common factor matrix and E_t is the idiosyncratic component with $\mathbb{E}(F_t) = 0$ and $\mathbb{E}(E_t) = 0$. This model is suited for well-structured tables of macroeconomic indicators, financial characteristics, and frames of pictures etc. In this paper, we are interested in recovering the loading spaces $\text{Span}(R)$ and $\text{Span}(C)$. Without loss of generality, we assume $R^\top R/p = I_{p_0}$ and $C^\top C/q = I_{q_0}$. The projection matrices onto $\text{Span}(R)$ and $\text{Span}(C)$ are then naturally $P_R = RR^\top/p$ and $P_C = CC^\top/q$.

Prior to the introduction of Matrix Elliptical Factor Model (MEFM), we first take a look at matrix elliptical distributions. A random matrix X of size $p \times q$ is matrix elliptical distributed if its characteristic function has the form $\varphi_X(T) = \exp[\text{tr}(iT^\top M)] \psi[\text{tr}(T^\top \Sigma T \Omega)]$ with $T: p \times q$, $M: p \times q$, $\Sigma: p \times p$, $\Omega: q \times q$, $\Sigma \succcurlyeq O$, $\Omega \succcurlyeq O$ and $\psi: [0, \infty) \rightarrow \mathbb{R}$. This distribution is denoted by $E_{p,q}(M, \Sigma \otimes \Omega, \psi)$, see Gupta and Nagar (2018) for details. An important observation given in Gupta and Varga (1994) shows that for $\text{rank}(\Sigma) = m$, $\text{rank}(\Omega) = n$, the random matrix $X \sim E_{p,q}(M, \Sigma \otimes \Omega, \psi)$ if and only if:

$$X \stackrel{d}{=} rAUB^\top + M,$$

where $U: m \times n$ and $\text{Vec}(U)$ is uniformly distributed on the unit sphere in \mathbb{R}^{mn} , r is a nonnegative random variable independent of U , $\Sigma = AA^\top$ and $\Omega = BB^\top$ are rank factorizations of Σ and Ω . The matrix Gaussian distributions and matrix t -distributions belong to the class of matrix elliptical distributions. In the article, in the definition of MEFM, we assume the factor F_t and noise E_t are from joint matrix elliptical distribution as in He et al. (2022), which is:

$$\begin{pmatrix} \text{Vec}(F_t) \\ \text{Vec}(E_t) \end{pmatrix} = r_t \begin{pmatrix} \Sigma_2^{1/2} \otimes \Sigma_1^{1/2} & 0 \\ 0 & \Omega_2^{1/2} \otimes \Omega_1^{1/2} \end{pmatrix} \frac{Z_t}{\|Z_t\|_2}, \quad (2.1)$$

where Z_t is a $(pq + p_0q_0)$ -dimensional isotropic Gaussian vector, while r_t is a positive random variable independent of Z_t . It is sometimes more convenient to separate the joint model into:

$$F_t = \frac{r_t}{\|Z_t\|_2} \Sigma_1^{1/2} Z_t^F \Sigma_2^{1/2}, \quad E_t = \frac{r_t}{\|Z_t\|_2} \Omega_1^{1/2} Z_t^E \Omega_2^{1/2},$$

with positive-definite transformation matrices Σ_1 of size $p_0 \times p_0$, Σ_2 of size $q_0 \times q_0$, Ω_1 of size $p \times p$ and Ω_2 of size $q \times q$. Z_t^F is a $p_0 \times q_0$ random matrix by taking the leading p_0q_0 elements of Z_t , while Z_t^E of size $p \times q$ consists of all the elements left. It is not hard to verify that F_t and E_t are matrix elliptical distributed, since $\|Z_t\|_2^2 = \|Z_t^F\|_F^2 + \|Z_t^E\|_F^2$ is independent of both $Z_t^F/\|Z_t^F\|_F$ and $Z_t^E/\|Z_t^E\|_F$.

Remark 2.1. Assuming the joint matrix elliptical distribution of F_t and E_t is to ensure distribution-free

signal-to-noise conditions. For example, if E_t has i.i.d. standard Gaussian elements, then $\|E_t\|_{op} = O_p((p \vee q)^{1/2})$. On the other hand, if E_t has i.i.d. $t(1)$ elements, then $\|E_t\|_{op} \geq \|E_t\|_\infty \asymp pq$. Assuming joint matrix elliptical distribution ensures simplicity, otherwise, the signal-to-noise conditions are distribution-dependent, and higher signal-to-noise ratio is naturally required for heavier-tailed noise case. See the same joint (vector) elliptical distribution assumption in [Fan et al. \(2018\)](#); [He et al. \(2022\)](#).

2.2 Manifold Principle Component Analysis

In this section, we introduce our Manifold Principle Component Analysis (MPCA) method for MEFM estimation. As a simple heuristic argument to see the robustness of MPCA, first consider $q = 1$ and then the matrix factor model degenerates to the vector case. The classical vector factor model would be written as:

$$y_t = Af_t + \epsilon_t, \quad t = 1, \dots, T,$$

where y_t is the $p \times 1$ observed vector, A is the $p \times p_0$ loading matrix, f_t is the $p_0 \times 1$ latent factor vector and ϵ_t is the $p \times 1$ noise vector. The classical PCA seeks the leading p_0 eigenvectors of the sample covariance matrix $\tilde{\Sigma} = \sum_t y_t y_t^\top / T$, which is easily influenced by outliers, as those y_t with larger norm naturally have larger influence on $\tilde{\Sigma}$.

It would be more robust to treat all y_t equally, in a sense that each y_t provides the same amount of subspace information. The Manifold PCA (MPCA) first finds the best subspace estimation \hat{A}_t for each y_t , which is the first eigenvector of the rank one matrix $y_t y_t^\top$. Then it seeks the ‘‘center’’ of all \hat{A}_t , which would be the leading eigenvectors of the average projection matrix $\hat{\Sigma} = \sum_t \hat{A}_t \hat{A}_t^\top / T$. It is exactly a distance-weighted sample covariance, namely:

$$\hat{\Sigma} = \sum_t \hat{A}_t \hat{A}_t^\top / T = \sum_t \frac{y_t y_t^\top}{y_t^\top y_t} / T.$$

Such degeneration towards vector factor model provides some basic insights for the robustness of our MPCA methods against heavy-tailed noises. If the data set $\{y_t, 1 \leq t \leq T\}$ is augmented to $\{y_i - y_j, 1 \leq i < j \leq T\}$, our method is then equivalent to calculating the leading eigenvectors of the multivariate Kendall’s τ matrix, which is also valid without moment conditions, see [He et al. \(2022\)](#) for details.

We then introduce the MPCA methods for matrix variate data. Assume first $p_0 = q_0 = r_0$, for each data matrix X_t , we give the best linear row/column space estimator for X_t , denoted by orthogonal matrices \hat{R}_t and \hat{C}_t respectively, which are the representatives of their own equivalent classes on the Grassmann manifolds $\mathcal{G}(p_0, p)$ and $\mathcal{G}(q_0, q)$. Then MPCA finds the ‘‘centers’’ of all $\text{Span}(\hat{R}_t)$ and $\text{Span}(\hat{C}_t)$ within their Grassmann manifolds respectively.

In the following section, we will show that for each X_t , the best linear subspace estimator \hat{R}_t and \hat{C}_t are the leading r_0 eigenvectors of $X_t X_t^\top$ and $X_t^\top X_t$ with respect to operator norm $\|\cdot\|_{op}$ loss in (2.2) below. Similarly, \hat{R}_t and \hat{C}_t are leading r_0 eigenvectors of $X_t P_C X_t^\top$ and $X_t^\top P_R X_t$ under Frobenius norm $\|\cdot\|_F$ loss if C and R are given respectively.

Then, for given linear space estimators \hat{R}_t and \hat{C}_t for each X_t , it is natural to find their ‘‘centers’’ on the Grassmann manifolds $\mathcal{G}(p_0, p)$ and $\mathcal{G}(q_0, q)$ as the final estimators. However, Grassmann manifolds

admit highly non-linear structures and direct sample averaging is not admissible. Fortunately, we show that the leading r_0 eigenvectors of the average projection matrices $\bar{P}_{\hat{R}_t} = \sum_t \hat{R}_t \hat{R}_t^\top / T$ and $\bar{P}_{\hat{C}_t} = \sum_t \hat{C}_t \hat{C}_t^\top / T$, denoted by \hat{R} / \sqrt{p} and \hat{C} / \sqrt{q} , could serve as the representatives of the Manifolds.

Remark 2.2. Although such manifold center intuition seems vivid, we have to be more careful with those degenerated cases where the best linear subspace approximation for each single matrix data is of lower dimensional than expected. For instance, if the factor matrix F_t is of dimension $p_0 \times q_0$ with $p_0 > q_0$, and we wish to find a p_0 -dimensional subspace $\text{Span}(\hat{R})$. The signal part $R F_t C^\top$ would be of rank $r_0 = q_0$, so it would be more natural to set \hat{R}_t as the leading q_0 left singular vectors of X_t , instead of p_0 . The algorithm could be slightly modified and performs equally well, but the intuition of manifold “center” no longer makes sense, as each \hat{R}_t is q_0 -dimensional while the \hat{R} we seek is p_0 -dimensional. That is to say, we are finding the p_0 -dimensional “centered” subspace among some q_0 -dimensional subspaces, hence we adopt the term degeneration.

2.3 Best Subspace Approximations

First, consider the best subspace approximation for a single matrix data X_t . We aim to find basis matrices \hat{R}_t and \hat{C}_t of dimension $p \times p_0$ and $q \times q_0$ respectively, and the $p_0 \times q_0$ compressed factor matrix \hat{F}_t such that $\hat{R}_t \hat{F}_t \hat{C}_t^\top$ is sufficiently close to the original X_t . It is then natural to solve the following optimization problem for some matrix norm $\|\cdot\|$,

$$(\hat{R}_t, \hat{F}_t, \hat{C}_t) = \arg \min_{R_t \in \mathcal{O}_{p,p_0}, C_t \in \mathcal{O}_{q,q_0}, F_t} \|X_t - R_t F_t C_t^\top\|. \quad (2.2)$$

For the Frobenius norm $\|\cdot\|_F$, it is well-known that if \hat{R}_t and \hat{C}_t are given, \hat{F}_t would simply be the projected value $\hat{R}_t^\top X_t \hat{C}_t$, see [He et al. \(2021b\)](#). After simple matrix manipulation, \hat{R}_t would be the leading eigenvectors of $X_t P_{\hat{C}_t} X_t^\top$ and \hat{C}_t would be the leading eigenvectors of $X_t^\top P_{\hat{R}_t} X_t$.

For the operator norm $\|\cdot\|_{op}$, unfortunately, a close form solution for \hat{F}_t even if R_t and C_t are given is vacant. However, the optimized value $\mathcal{M}(R_t, C_t) = \|X_t - R_t \hat{F}_t C_t^\top\|_{op}$ has a closed form for $\hat{F}_t = \arg \min_{F_t} \|X_t - R_t F_t C_t^\top\|_{op}$, if the largest singular values of $X_t - R_t \hat{F}_t C_t^\top$ do not coincide so that the operator norm $\|\cdot\|_{op}$ is differentiable, which is:

$$\mathcal{M}(R_t, C_t) = \|X_t - R_t \hat{F}_t C_t^\top\|_{op} = \sigma_{R_t} \vee \sigma_{C_t},$$

where $\sigma_{R_t}^2$ and $\sigma_{C_t}^2$ are respectively the largest singular values of the matrices Σ_{R_t} and Σ_{C_t} , defined as

$$\Sigma_{R_t} = (I - P_{R_t}) X_t, \quad \Sigma_{C_t} = (I - P_{C_t}) X_t^\top.$$

We could minimize σ_{R_t} and σ_{C_t} separately. It is then straightforward that \hat{R}_t and \hat{C}_t are the leading p_0 left and q_0 right singular vectors of the matrix data X_t . In the end, as the optimization problem is sufficiently continuous and operator norm $\|\cdot\|_{op}$ is differentiable almost everywhere except for a zero Lebesgue measure set, the above solutions would be numerically valid.

2.4 MPCA algorithms for MEFM

In this section, we give the details of the MPCA algorithms. We first discuss the operator loss approximation case, naming this variant as MPCA_{op} . As discussed earlier, MPCA_{op} first acquires the best linear subspace approximation \widehat{R}_t and \widehat{C}_t for each data matrix X_t by singular value decompositions. For non-degenerated cases namely $r_0 = p_0 = q_0$, \widehat{R}_t and \widehat{C}_t would be the leading r_0 left and right singular vectors of X_t , which are the representatives of elements on the Grassmann manifolds $\mathcal{G}(p_0, p)$ and $\mathcal{G}(q_0, q)$ respectively. Then, MPCA_{op} finds the centers by minimizing the projection metrics on Grassmann manifolds:

$$\widehat{R}_{op}/\sqrt{p} = \arg \min_{R^\top R = I_{p_0}} \sum_{t=1}^T \|RR^\top - \widehat{R}_t \widehat{R}_t^\top\|_F^2, \quad \widehat{C}_{op}/\sqrt{q} = \arg \min_{C^\top C = I_{q_0}} \sum_{t=1}^T \|CC^\top - \widehat{C}_t \widehat{C}_t^\top\|_F^2,$$

which is analogous to the physical notion of barycenter. Without loss of generality, we only focus on discussion of \widehat{R} here. Denote $P_R = RR^\top$ and $P_{\widehat{R}_t} = \widehat{R}_t \widehat{R}_t^\top$, then we have:

$$\sum_t \|RR^\top - \widehat{R}_t \widehat{R}_t^\top\|_F^2 = \sum_t \text{tr}(P_R) + \sum_t \text{tr}(P_{\widehat{R}_t}) - 2\text{tr} \left[P_R \left(\sum_t P_{\widehat{R}_t} \right) \right].$$

Algorithm 1 MPCA algorithm under the operator norm loss.

Require:

- The set of all data matrices, $\{X_t\}$;
- Compression dimensions, $p_0 \leq r$ and $q_0 \leq r$;

Ensure:

- Estimators by MPCA_{op} , \widehat{R}_{op} and \widehat{C}_{op} ;
 - 1: Acquire the best linear subspace estimations \widehat{R}_t and \widehat{C}_t for each X_t . For MPCA_{op} , \widehat{R}_t and \widehat{C}_t are the leading $r_0 = p_0 \wedge q_0$ eigenvectors of $X_t X_t^\top$ and $X_t^\top X_t$;
 - 2: The $\widehat{R}_{op}/\sqrt{p}$ and $\widehat{C}_{op}/\sqrt{q}$ are the leading p_0 and q_0 eigenvectors of the average projection matrices $\sum_t \widehat{R}_t \widehat{R}_t^\top / T$ and $\sum_t \widehat{C}_t \widehat{C}_t^\top / T$;
 - 3: **return** $\widehat{R}_{op}, \widehat{C}_{op}$.
-

The first two terms on the right hand side are fixed, so we are actually maximizing the last term, namely $\mathcal{L}(R) = \text{tr} \left[R^\top \left(\sum_t P_{\widehat{R}_t} \right) R \right]$. It is a classical eigenvalue problem and $\widehat{R}_{op}/\sqrt{p}$ would be the leading p_0 eigenvectors of the average projection matrix $\sum_t P_{\widehat{R}_t} / T$.

As for the degenerated case where $p_0 \neq q_0$, without loss generality we assume $p_0 > q_0$, then \widehat{R}_t and \widehat{C}_t are the leading $r_0 = q_0$ left and right singular vectors of X_t . Solve the same optimization problem and $\widehat{R}_{op}/\sqrt{p}$, $\widehat{C}_{op}/\sqrt{q}$ are still the leading p_0, q_0 eigenvectors of the average projection matrices $\sum_t P_{\widehat{R}_t} / T$, $\sum_t P_{\widehat{C}_t} / T$ respectively. It is easy to see that $\widehat{C}_{op}/\sqrt{q}$ is exactly the same as in the non-degenerated case. As for \widehat{R}_t , it is of size $p \times q_0$. It is no longer a representative of some element in $\mathcal{G}(p_0, p)$, thus the manifold center intuition no longer holds. However similar geometric interpretation is still somehow valid: each \widehat{R}_t corresponds to a q_0 -dimensional subspace, and with some principal angle related arguments, $\text{tr}(P_{\widehat{R}_t} P_R)$ still gives the magnitude of deviation of q_0 -dimensional $\text{Span}(\widehat{R}_t)$ from the p_0 -dimensional $\text{Span}(R)$. It is obvious that MPCA_{op} needs $p_0 \vee q_0 \leq r = p \wedge q$, as we are seeking

for lower dimensional column and row subspaces, and the right hand side is the maximal rank of the original data matrices $\{X_t\}$. The detailed procedures for MPCA_{op} is summarized in Algorithm 1.

We now discuss the Frobenius loss case, naming this variant as MPCA_F . Under Frobenius loss, \widehat{R}_t would be the leading r_0 eigenvectors of $X_t P_C X_t^\top$ if C is given and \widehat{C}_t would be the leading r_0 eigenvectors of $X_t^\top P_R X_t$ if R is given. Then MPCA_F takes the leading eigenvectors of the average projection matrices similarly. Note that iterative procedure is necessary as C and R is unavailable at the beginning. For initial value, the estimators by MPCA_{op} can be adopted as a warm start. The detailed procedures for MPCA_F is summarized in Algorithm 2.

Algorithm 2 MPCA algorithm under the Frobenius norm loss.

Require:

- The set of all data matrices, $\{X_t\}$;
- Compression dimensions, $p_0 \leq r$ and $q_0 \leq r$;

Ensure:

- Estimators by MPCA_F , \widehat{R}_F and \widehat{C}_F ;
 - 1: Use the result of MPCA_{op} as a warm start, denoted by $\widehat{R}^{(0)}$ and $\widehat{C}^{(0)}$;
 - 2: Assume we have acquired $\widehat{R}^{(i)}$ and $\widehat{C}^{(i)}$, then $\widehat{R}_t^{(i+1)}$ and $\widehat{C}_t^{(i+1)}$ are the leading $r_0 = p_0 \wedge q_0$ eigenvectors of $X_t P_{\widehat{C}^{(i)}} X_t^\top$ and $X_t^\top P_{\widehat{R}^{(i)}} X_t$ respectively;
 - 3: Then $\widehat{R}^{(i+1)}/\sqrt{p}$ and $\widehat{C}^{(i+1)}/\sqrt{q}$ are the leading p_0 and q_0 eigenvectors of the average projection matrices $\sum_t \widehat{R}_t^{(i+1)} (\widehat{R}_t^{(i+1)})^\top / T$ and $\sum_t \widehat{C}_t^{(i+1)} (\widehat{C}_t^{(i+1)})^\top / T$ respectively; iterate until convergence to $\widehat{R}_F, \widehat{C}_F$;
 - 4: **return** $\widehat{R}_F, \widehat{C}_F$.
-

3 Theoretical Results

In this section, we present the theoretical properties of the estimators by MPCA, and throughout this section, the number of factors p_0 and q_0 are treated as given. The determination of factor numbers p_0, q_0 are left to Section 4.

3.1 Expected Projection Matrix

Prior to presenting the consistency of our MPCA estimators, we first give some intuitions on why the algorithms work. For clearer illustration, we only analyze \widehat{R}_{op} by MPCA_{op} . Recall that the model is $X_t = R F_t C^\top + E_t$, while \widehat{R}_t is the leading r_0 left singular vectors of X_t . In the end, $\widehat{R}_{op}/\sqrt{p}$ is acquired by taking the leading p_0 eigenvectors of the average projection matrix $\bar{P}_{\widehat{R}_t}$. Obviously, the algorithm relies heavily on the concentration of average projection matrix $\bar{P}_{\widehat{R}_t}$ to its expected version $\mathbb{E}P_{\widehat{R}_t}$. The algorithms could be justified as long as we show that:

1. The average projection matrix $\bar{P}_{\widehat{R}_t}$ converges to the expected version $\mathbb{E}P_{\widehat{R}_t}$ at a rate of \sqrt{T} .
2. The leading eigenvectors of the expected version $\mathbb{E}P_{\widehat{R}_t}$ give us $\text{Span}(R)$ as desired.

As for the first part, with the help of matrix concentration inequalities in [Tropp \(2012\)](#), we have:

Lemma 3.1 (\sqrt{T} -Convergence). For i.i.d. random projection matrices $P_{\widehat{R}_t}$ with dimension p , for all $x \geq 0$, the following concentration inequality holds,

$$\mathbb{P} \left\{ \left\| \sum_{t=1}^T (P_{\widehat{R}_t} - \mathbb{E}P_{\widehat{R}_t}) \right\|_{op} \geq x \right\} \leq p \cdot e^{-x^2/8T}.$$

Although we are quite satisfied with this \sqrt{T} -consistency result for finite-dimensional matrix data, the haunting dimensional factor p of matrix concentration inequalities would give exploding bounds if the dimension p tends to infinity. Fortunately, in this case of random projection matrices, we are able to shrink the dimensional factor p to r_0 via intrinsic dimension arguments. As r_0 remains fixed as p goes to infinity, dimension-free convergence could be acquired.

As for the second part, we claim that $\text{Span}(R)$ and $\text{Span}(R^\perp)$ are invariant subspaces of the expected projection matrix $\mathbb{E}P_{\widehat{R}_t}$ if the noise E_t is left spherical. Matrix spherical distribution can be viewed as a special case of matrix elliptical distribution. The random matrix X is left spherical if $X \sim E_{p,q}(0, I \otimes \Omega, \psi_l)$, right spherical if $X \sim E_{p,q}(0, \Sigma \otimes I, \psi_r)$ and spherical if $X \sim E_{p,q}(0, I \otimes I, \psi_s)$. If E_t is left spherical, then $E_t \stackrel{d}{=} WE_t, \forall W \in \mathcal{O}_{p,p}$. Right spherical and spherical distributions have similar properties accordingly. Random matrices with i.i.d. centered Gaussian or t_v elements are matrix spherically distributed, see [Gupta and Nagar \(2018\)](#) for details.

Lemma 3.2 (Invariant Subspaces). For joint matrix elliptical data $X_t = RF_tC^\top + E_t$ as in 2.1, let $P_{\widehat{R}_t} = \widehat{R}_t\widehat{R}_t^\top$, where \widehat{R}_t is the leading $r_0 = p_0 \wedge q_0$ eigenvectors of $X_tX_t^\top$. If E_t is left spherical, then $\text{Span}(R)$ and $\text{Span}(R^\perp)$ are invariant subspaces of $\mathbb{E}P_{\widehat{R}_t}$.

The joint matrix elliptical model here is more of a burden instead of blessing. In fact, the conclusion is more straightforward if F_t and E_t are independent and could be of independent interest. The combination of Lemmas 3.1 and 3.2 theoretically justifies the validity of the proposed MPCA methods: the expected projection matrix contains adequate subspace information, while the matrix concentration to it is guaranteed by the compactness of the projection matrices.

3.2 Technical Assumptions

In this section, we give some technical assumptions to establish the convergence rates of the estimators by MPCA.

Assumption A (Joint Matrix Elliptical Model). We assume matrix elliptical factor model as:

$$X_t = RF_tC^\top + E_t, \quad t = 1, \dots, T,$$

$$\begin{pmatrix} \text{Vec}(F_t) \\ \text{Vec}(E_t) \end{pmatrix} = r_t \begin{pmatrix} \Sigma_2^{1/2} \otimes \Sigma_1^{1/2} & 0 \\ 0 & \Omega_2^{1/2} \otimes \Omega_1^{1/2} \end{pmatrix} \frac{Z_t}{\|Z_t\|_2},$$

where Z_t is a $(pq + p_0q_0)$ -dimensional isotropic Gaussian vector, r_t is a positive random variable independent of Z_t , with $(pq)^{-1/2}r_t = O_p(1)$ as $p, q \rightarrow \infty$. It is sometimes more convenient to separate the

joint model into:

$$F_t = \frac{r_t}{\|Z_t\|_2} \Sigma_1^{1/2} Z_t^F \Sigma_2^{1/2}, \quad E_t = \frac{r_t}{\|Z_t\|_2} \Omega_1^{1/2} Z_t^E \Omega_2^{1/2},$$

with Σ_1 of size $p_0 \times p_0$, Σ_2 of size $q_0 \times q_0$, Ω_1 of size $p \times p$ and Ω_2 of size $q \times q$. Z_t^F is a $p_0 \times q_0$ random matrix made by leading $p_0 q_0$ elements of Z_t , while Z_t^E of size $p \times q$ consists of all the elements left.

Assumption B (Strong Factor Conditions). We assume $R^\top R/p = I_{p_0}$ and $C^\top C/q = I_{q_0}$. In addition, there exist positive constants c_1 and C_1 such that $c_1 \leq \lambda_{p_0}(\Sigma_1) \leq \lambda_1(\Sigma_1) \leq C_1$, $c_1 \leq \lambda_{q_0}(\Sigma_2) \leq \lambda_1(\Sigma_2) \leq C_1$ as $p, q \rightarrow \infty$.

Assumption C (Regular Noise Conditions). We assume there exist positive constants c_2 and C_2 such that $c_2 \leq \lambda_p(\Omega_1) \leq \lambda_1(\Omega_1) \leq C_2$, $c_2 \leq \lambda_q(\Omega_2) \leq \lambda_1(\Omega_2) \leq C_2$ as $p, q \rightarrow \infty$.

The convergence relies heavily on matrix concentration results. The independence between $\{X_t\}$ in Assumption A could extend readily to weak dependence by matrix concentration results such as matrix Azuma inequality, see Tropp (2012), Tropp (2015) for details. Assumption B and C are standard in large-dimensional factor models. In addition, the joint matrix elliptical distribution assumption is only for the convenience of theoretical analysis, while empirical experiments show that the MPCA methods are not sensitive to the elliptical assumption.

3.3 Consistency of Manifold PCA

Theorem 3.3 (Consistency of MPCA_{op}). For MPCA_{op} , under Assumption A to C, there exist $p_0 \times p_0$ orthonormal matrix H_R and $q_0 \times q_0$ orthonormal matrix H_C such that:

$$\|\widehat{R}_{op} - RH_R\|_F^2/p = O_p(T^{-1} + p^{-1/2} + q^{-1/2}),$$

$$\|\widehat{C}_{op} - CH_C\|_F^2/q = O_p(T^{-1} + p^{-1/2} + q^{-1/2}).$$

As MPCA methods rely heavily on the concentration of T projection matrices, the convergence rate would be at most T^{-1} . It is slower than α -PCA from Chen and Fan (2021) and PE from Yu et al. (2021) with the rate $(Tq)^{-1}$ (or $(Tp)^{-1}$) when estimating R (or C) under strong signal conditions, which are comparable to taking each column (or row) as individual observation. The inefficiency of MPCA methods comes from the fact that by taking each projection matrix as individual observation would lose information especially when each matrix observation X_t is of large dimensions. However, as we will see in the simulation study, MPCA performs comparably to the classical methods for Gaussian noise, while the compactness of the projection matrices ensures the good performance of MPCA even for noises without any moments. As a result, they could be potential replacements of classical methods for data with heavier-tailed noise.

For MPCA_F method, we further discuss how the information of column factor loading matrix C would help to estimate R , which is named as the projection effect in this work. Estimation of C can be discussed in a similar way. Recall that for MPCA_F , $\widehat{R}_t^{(i)}$ would be the leading $r_0 = p_0 \wedge q_0$ eigenvalues of $X_t P_{\widehat{C}^{(i-1)}} X_t^\top$ if $\widehat{C}^{(i-1)}$ is given. Let $C^{(i-1)} = \widehat{C}^{(i-1)} / \sqrt{q}$ for notational simplicity. We focus on the projected matrix model $X_t C^{(i-1)} = R F_t C^\top C^{(i-1)} + E_t C^{(i-1)}$, and $\widehat{R}_t^{(i)}$ would exactly be the estimator by the MPCA_{op} to the projected data set $\{X_t C^{(i-1)}\}$.

The difference with/without projection lies in the signal-to-noise ratio level. Consider the extreme case where the true value C is known, for $X_t C / \sqrt{q} = q^{1/2} R F_t + E_t C / \sqrt{q}$, the projection does no harm to the signal size while compressing the noise to lower-dimensional $E_t C / \sqrt{q}$. It is then foreseeable that we could increase the signal-to-noise ratio via projection by some $\widehat{C}^{(i-1)}$ sufficiently close to C , keeping the signal size almost unchanged. It is ensured by assuming $\sigma_{q_0}(C^\top \widehat{C}^{(i-1)})/q = c > 0$, which is a rather mild condition.

Theorem 3.4 (Projection Effect of MPCA_F). For each iteration step of MPCA_F , under Assumption **A** to **C**, given $\widehat{C}^{(i-1)}$, if we assume that $\sigma_{q_0}(C^\top \widehat{C}^{(i-1)})/q > 0$, then there exists $p_0 \times p_0$ orthonormal matrix H_R such that:

$$\left\| \widehat{R}^{(i)} - R H_R \right\|_F^2 / p = O_p \left(T^{-1} + q^{-1/2} \right).$$

Similarly, given $\widehat{R}^{(i-1)}$, if we assume that $\sigma_{p_0}(R^\top \widehat{R}^{(i-1)})/p > 0$, then there exists $q_0 \times q_0$ orthonormal matrix H_C such that:

$$\left\| \widehat{C}^{(i)} - C H_C \right\|_F^2 / p = O_p \left(T^{-1} + p^{-1/2} \right).$$

As we take the estimator MPCA_{op} as the initial estimate, which is shown to be consistent under Assumption **A** to **C** by Theorem 3.3, we have $\sigma_{q_0}(C^\top \widehat{C}^{(0)})/q > 0$ and $\sigma_{p_0}(R^\top \widehat{R}^{(0)})/p > 0$ with probability tending to 1.

3.4 Factor and Common Component Matrices

After the loading matrices being determined, the factor matrix F_t can be naturally estimated by $\widehat{F}_t = \widehat{R}^\top X_t \widehat{C} / (pq)$, and the common component matrix $S_t = R F_t C^\top$ be estimated by $\widehat{S}_t = \widehat{R} \widehat{F}_t \widehat{C}^\top$.

Corollary 3.1 (Consistency of Factor and Common Component Matrices). Suppose there exist $p_0 \times p_0$ orthonormal matrix H_R and $q_0 \times q_0$ orthonormal matrix H_C such that for $\varepsilon_R = \widehat{R} - R H_R$ and $\varepsilon_C = \widehat{C} - C H_C$, we have $\|\varepsilon_R / \sqrt{p}\|_{op} = o_p(1)$ and $\|\varepsilon_C / \sqrt{q}\|_{op} = o_p(1)$, then:

$$\left\| \widehat{F}_t - H_R^\top F_t H_C \right\|_{op} = O_p \left(\left\| \frac{\varepsilon_R}{\sqrt{p}} \right\|_{op} + \left\| \frac{\varepsilon_C}{\sqrt{q}} \right\|_{op} + (pq)^{-1/2} \right),$$

$$\left\| \widehat{S}_t - S_t \right\|_{op} / \sqrt{pq} = O_p \left(\left\| \frac{\varepsilon_R}{\sqrt{p}} \right\|_{op} + \left\| \frac{\varepsilon_C}{\sqrt{q}} \right\|_{op} + (pq)^{-1/2} \right).$$

Here $\|\varepsilon_R / \sqrt{p}\|_{op} = o_p(1)$ and $\|\varepsilon_C / \sqrt{q}\|_{op} = o_p(1)$ are direct consequences of Theorem 3.3 under Assumptions **A** to **C**, so we claim the consistency of factor and common component matrices.

4 Determining the Factor Numbers

In the last section, the factor number is assumed to be known in advance, while in practice, the factor numbers p_0 and q_0 need to be determined. We propose a natural criterion by calculating eigenvalue-ratios (ER) of the average projection matrices, under both MPCA_{op} and MPCA_F . The corresponding algorithms are named as MER_{op} and MER_F respectively. Unlike existing eigenvalue-ratio methods

based on covariance-type matrices as in [Chen and Fan \(2021\)](#) and [Yu et al. \(2021\)](#), MER_{op} and MER_F are clearly free of moment-constraints. For MER_{op} , first determine the compression rank \hat{r}_0 by averaging $\hat{r}_{0,t}$ acquired from each data matrix X_t , that is:

$$\hat{r}_{0,t} = \arg \max_{j \leq r_{\max}} \frac{\sigma_j(X_t)}{\sigma_{j+1}(X_t)}, \quad \hat{r}_0 = \lfloor \sum_{t=1}^T \hat{r}_{0,t} / T + \frac{1}{2} \rfloor,$$

where $\lfloor x + \frac{1}{2} \rfloor$ means rounding x to the nearest integer. Then p_0 and q_0 are estimated by:

$$\hat{p}_0^{op} = \arg \max_{j \leq r_{\max}} \frac{\lambda_j(\bar{P}_{\tilde{R}_t})}{\lambda_{j+1}(\bar{P}_{\tilde{R}_t})}, \quad \hat{q}_0^{op} = \arg \max_{j \leq r_{\max}} \frac{\lambda_j(\bar{P}_{\tilde{C}_t})}{\lambda_{j+1}(\bar{P}_{\tilde{C}_t})}. \quad (4.1)$$

where r_{\max} is predetermined value larger than p_0, q_0 , while $\bar{P}_{\tilde{R}_t}, \bar{P}_{\tilde{C}_t}$ are the average projection matrices by taking the leading \hat{r}_0 left and right singular vectors of each X_t respectively.

Remark 4.1. In fact, accurate estimation of \hat{r}_0 is not necessary for MER_{op} , we could still get comparable results from 4.1 even if $\hat{r}_0 \neq r_0$. However, since each data matrix contains at most r_0 -dimensional subspace information, pre-estimation of r_0 could stabilize the algorithm. Once r_0 has been correctly estimated, \tilde{R}_t would be exactly \hat{R}_t in MPCA_{op} . Further analysis in supplementary materials ensures that $\lambda_{p_0}(\mathbb{E}P_{\hat{R}_t}) \geq c > 0$, $\lambda_{p_0+1}(\mathbb{E}P_{\hat{R}_t}) \rightarrow 0$ while $\|\bar{P}_{\tilde{R}_t} - \mathbb{E}P_{\hat{R}_t}\|_{op} \rightarrow 0$ as $T, p, q \rightarrow \infty$ under Assumption A to C, which theoretically justifies MER_{op} .

Algorithm 3 MER_{op} estimators of the pair of the factor numbers

Require:

- The set of all data matrices, $\{X_t\}$;
- Maximum number, r_{\max} ;

Ensure:

- MER_{op} estimators, \hat{p}_0^{op} and \hat{q}_0^{op} ;
 - 1: Acquire compression dimension \hat{r}_0 by averaging $\hat{r}_{0,t}$ from each data matrix X_t , where $\hat{r}_{0,t} = \arg \max_{j \leq r_{\max}} \sigma_j(X_t) / \sigma_{j+1}(X_t)$ and $\hat{r}_0 = \lfloor \sum_{t=1}^T \hat{r}_{0,t} / T + \frac{1}{2} \rfloor$;
 - 2: Acquire the best linear subspace estimations \tilde{R}_t and \tilde{C}_t for each X_t , which are the leading \hat{r}_0 eigenvectors of $X_t X_t^\top$ and $X_t^\top X_t$;
 - 3: Calculate the average projection matrices $\bar{P}_{\tilde{R}_t}, \bar{P}_{\tilde{C}_t}$ from \tilde{R}_t and \tilde{C}_t . Determine \hat{p}_0^{op} and \hat{q}_0^{op} by finding the largest eigenvalue-ratio from $\lambda_j(\bar{P}_{\tilde{R}_t}) / \lambda_{j+1}(\bar{P}_{\tilde{R}_t})$ and $\lambda_j(\bar{P}_{\tilde{C}_t}) / \lambda_{j+1}(\bar{P}_{\tilde{C}_t})$ for $j \leq r_{\max}$;
 - 4: **return** $\hat{p}_0^{op}, \hat{q}_0^{op}$.
-

Theorem 4.2 (Consistency of MER_{op} estimators). Under Assumption A to C, assume the maximum number $r_{\max} \geq p_0 \vee q_0$, as $T, p, q \rightarrow \infty$,

$$\mathbb{P}(\hat{p}_0^{op} = p_0) \rightarrow 1, \quad \mathbb{P}(\hat{q}_0^{op} = q_0) \rightarrow 1.$$

Similarly, we could use the average projection matrices from MPCA_F to increase accuracy. Now

that estimating p_0 requires information of C , and estimating q_0 requires information of R , iterations are naturally needed, and the result from MER_{op} estimators could be used as a warm start.

Algorithm 4 MER_F estimators of the pair of the factor numbers

Require:

- The set of all data matrices, $\{X_t\}$;
- Maximum number, r_{\max} ;

Ensure:

- MER_F estimators, \hat{p}_0^F and \hat{q}_0^F ;
 - 1: Use the MER_{op} estimators as a warm start, denoted by $\hat{p}_0^{(0)}, \hat{q}_0^{(0)}$;
 - 2: Given compression dimensions $\hat{p}_0^{(i)}, \hat{q}_0^{(i)}$, acquire $\tilde{R}_F^{(i)}$ and $\tilde{C}_F^{(i)}$ from MPCA_F ;
 - 3: Acquire the best linear subspace estimations $\tilde{R}_t^{(i+1)}$ and $\tilde{C}_t^{(i+1)}$ for each X_t , which are the leading $\hat{r}_0^{(i)} = \hat{p}_0^{(i)} \wedge \hat{q}_0^{(i)}$ eigenvectors of $X_t P_{\tilde{C}_F^{(i)}} X_t^\top$ and $X_t^\top P_{\tilde{R}_F^{(i)}} X_t$ respectively;
 - 4: Calculate the average projection matrices $\bar{P}_{\tilde{R}_t}^{(i+1)}, \bar{P}_{\tilde{C}_t}^{(i+1)}$ from $\tilde{R}_t^{(i+1)}$ and $\tilde{C}_t^{(i+1)}$. Determine $\hat{p}_0^{(i+1)}$ and $\hat{q}_0^{(i+1)}$ by finding the largest eigenvalue-ratio from $\lambda_j(\bar{P}_{\tilde{R}_t}^{(i+1)})/\lambda_{j+1}(\bar{P}_{\tilde{R}_t}^{(i+1)})$ and $\lambda_j(\bar{P}_{\tilde{C}_t}^{(i+1)})/\lambda_{j+1}(\bar{P}_{\tilde{C}_t}^{(i+1)})$ for $j \leq r_{\max}$; iterate until convergence to \hat{p}_0^F, \hat{q}_0^F ;
 - 5: **return** \hat{p}_0^F, \hat{q}_0^F .
-

Theoretical analysis of MER_F is challenging due to the iteration procedure, thankfully the initial step taken from MER_{op} has already been consistent under Assumption A to C. As shown in simulations, MER_F benefits from the same projection technique as in MPCA_F and turns out to be more accurate than MER_{op} in finite-sample performances.

5 Simulation Results

In this section, we investigate the finite-sample performances of MPCA algorithms by generating synthetic datasets. The observed data matrices are generated as $X_t = RF_t C^\top + E_t$ from moderate noise regime, by rescaling signal and noise to the same scale.

5.1 Data Generation

To generate observations from the model $X_t = RF_t C^\top + E_t, t = 1, \dots, T$, we set $p_0 = q_0 = 3$, draw the entries of R and C from independent standard Gaussian distribution, and let:

$$F_t = \Omega \times F_{t-1} + \sqrt{1 - \phi^2} \times U_t, \quad U_t \stackrel{i.i.d}{\sim} \mathcal{MN}(0, I_{p_0}, I_{q_0}).$$

$$E_t = \psi \times E_{t-1} + \sqrt{1 - \psi^2} \times s_E \times \Omega_1^{1/2} V_t \Omega_2^{1/2},$$

where $V_t = \gamma W_t$ and the elements of W_t are generated by independent standard centered Gaussian, t_v , skewed- t_v and α -stable distributions. The rescaling constant γ is to get comparable signal and noise level. In fact, if W_t consists of independent standard centered Gaussian random variables, the signal part $\|RF_t C^\top\|_{op} \asymp (pq)^{1/2}$ while $\|W_t\|_{op} \asymp (p \vee q)^{1/2}$, thus by setting $\gamma = (p \wedge q)^{1/2}$ we get comparable

signal and noise level. On the other hand, if W_t consists of independent t_1 random variables, it holds $\|W_t\|_{op} \gtrsim pq$, then we need to set $\gamma = (pq)^{-1/2}$.

The pair of dimensions (p, q) are chosen from the set $\{(20, 20), (20, 100), (100, 100)\}$, the sample size T is set to be $3(pq)^{1/2}$ and Ω_1, Ω_2 are set to be matrices with ones on the diagonal, and $1/p, 1/q$ on the off-diagonal respectively. In addition, the parameters ϕ and ψ control temporal correlation and are set as $\phi = \psi = 1/10$, while s_E is the noise scaling constant chosen from $\{1, 1.5, 2\}$. We only show the cases with $s_E = 1$ in this section, and the rest are left to the supplementary materials. Elements of V_t are drawn independently from standard Gaussian, t_3, t_1, α -stable distribution ($\alpha = 1.8$, skewness parameter $\beta = 0$), and skewed- t_3 distribution (standard deviation $\sigma = \sqrt{3}$, skewness parameter $\nu = 2$) respectively, while we set $\gamma = (pq)^{-1/2}$ for t_1 distribution and $\gamma = (p \wedge q)^{1/2}$ for the rest distributions. We generate α -stable distribution by Python package `scipy.stats`, and skewed- t_3 distribution by Python package `sstudentt`. All simulation results reported here are based on 100 replications.

5.2 Estimation of Loading Spaces

We first compare the performances of MPCA algorithms with those of $(2D)^2$ -PCA by [Zhang and Zhou \(2005\)](#) and PE method by [Yu et al. \(2021\)](#) in terms of estimating loading spaces. In fact, $(2D)^2$ -PCA is equivalent to α -PCA from [Chen and Fan \(2021\)](#) with $\alpha = -1$, whose empirical performances corresponding to $\alpha \in \{-1, 0, 1\}$ are comparable as shown in [Yu et al. \(2021\)](#). To measure the difference between the estimated \hat{R} and the true loading R , we used the scaled projection metric as in [Yu et al. \(2021\)](#), which is defined as:

$$\mathcal{D}(\hat{R}, R) = \left(1 - \frac{1}{p_0} \text{tr}(P_{\hat{R}} P_R)\right)^{1/2} = (2p_0)^{-1/2} \|P_{\hat{R}} - P_R\|_F,$$

so it is straightforward that $\mathcal{D}(\hat{R}, R)$ is always between 0 (corresponding to $\text{Span}(\hat{R}) = \text{Span}(R)$) and 1 (corresponding to $\text{Span}(\hat{R})$ and $\text{Span}(R)$ are orthogonal). $\mathcal{D}(\hat{C}, C)$ can be defined similarly.

Table 1 shows the averaged estimation errors of factor loadings with standard deviations in parentheses under different noise distributions with $s_E = 1$. Simulation results with $s_E \in \{1.5, 2\}$ are reported in Table 6 and 7 in the supplementary materials. First, it is observed that the projection effect of MPCA_F and PE is obvious for large-dimensional matrix factor analysis in finite-samples. The projected MPCA_F and PE almost always show advantages over MPCA_{op} and $(2D)^2$ -PCA, which in fact correspond to their non-projected versions. For the cases with Gaussian noise, the PE method achieves the best performances, while MPCA_F performs comparably. However, for heavy-tailed noises it is a completely different picture. MPCA_F shows great advantage over PE under t_3, t_1 and α -stable noises. It is foreseeable since MPCA methods require no moment conditions. Under relatively small noise scale, MPCA_{op} shows comparable performances as MPCA_F , but the latter benefits greatly from the projection effect and is more robust against larger noise scale, as shown in Table 6 and Table 7. In addition, by comparing the results under t_3 and skewed- t_3 noise, we observe that skewness does almost no harm to MPCA methods, while increasing the estimation errors of $(2D)^2$ -PCA and PE. To summarize, both MPCA_F and PE benefit greatly from the projection effect, which is essential in large-dimensional matrix factor analysis. MPCA methods perform comparably with $(2D)^2$ -PCA and PE under light-tailed noises, but

Table 1: Means and standard deviations (in parentheses) of $\mathcal{D}(\widehat{R}, R)$ and $\mathcal{D}(\widehat{C}, C)$ over 100 replications with $s_E = 1$ and $T = 3(pq)^{1/2}$. Here MPCA_{op} and MPCA_F stands for Manifold PCA methods; $(2D)^2$ -PCA is from [Zhang and Zhou \(2005\)](#), it is equivalent to α -PCA by [Chen and Fan \(2021\)](#) with $\alpha = -1$; PE stands for the projected estimation by [Yu et al. \(2021\)](#).

Distribution	Evaluation	p	q	MPCA_{op}	MPCA_F	$(2D)^2$ -PCA	PE
Gaussian	$\mathcal{D}(\widehat{R}, R)$	20	20	(0.3024,0.1272)	(0.1154,0.0233)	(0.2007,0.1147)	(0.0833,0.0179)
		20	100	(0.4510,0.1039)	(0.0402,0.0046)	(0.1375,0.0756)	(0.0234,0.0030)
		100	100	(0.0878,0.0226)	(0.0426,0.0025)	(0.0632,0.0173)	(0.0337,0.0024)
	$\mathcal{D}(\widehat{C}, C)$	20	20	(0.3005,0.1237)	(0.1170,0.0239)	(0.1807,0.1061)	(0.0838,0.0182)
		20	100	(0.0694,0.0073)	(0.0665,0.0058)	(0.0545,0.0067)	(0.0521,0.0059)
		100	100	(0.0891,0.0240)	(0.0424,0.0027)	(0.0629,0.0172)	(0.0334,0.0027)
t_3	$\mathcal{D}(\widehat{R}, R)$	20	20	(0.5145,0.0891)	(0.1941,0.0569)	(0.5678,0.1202)	(0.3077,0.2194)
		20	100	(0.5143,0.0682)	(0.0594,0.0094)	(0.5105,0.0870)	(0.0867,0.1413)
		100	100	(0.3184,0.1156)	(0.0662,0.0043)	(0.5638,0.1011)	(0.1864,0.2356)
	$\mathcal{D}(\widehat{C}, C)$	20	20	(0.4925,0.0907)	(0.1943,0.0578)	(0.5338,0.1159)	(0.3018,0.2037)
		20	100	(0.1239,0.0159)	(0.0998,0.0095)	(0.1732,0.1353)	(0.1379,0.1400)
		100	100	(0.2927,0.1108)	(0.0651,0.0047)	(0.5619,0.1022)	(0.1923,0.2420)
t_1	$\mathcal{D}(\widehat{R}, R)$	20	20	(0.0524,0.0130)	(0.0429,0.0061)	(0.7613,0.1322)	(0.7647,0.1738)
		20	100	(0.0328,0.0081)	(0.0198,0.0028)	(0.8076,0.1382)	(0.8175,0.1893)
		100	100	(0.0123,0.0009)	(0.0130,0.0007)	(0.9627,0.0596)	(0.9698,0.0668)
	$\mathcal{D}(\widehat{C}, C)$	20	20	(0.0525,0.0110)	(0.0430,0.0065)	(0.7569,0.1423)	(0.7638,0.1808)
		20	100	(0.0240,0.0023)	(0.0270,0.0023)	(0.8831,0.1620)	(0.8866,0.2009)
		100	100	(0.0121,0.0009)	(0.0130,0.0007)	(0.9637,0.0624)	(0.9681,0.0693)
α -stable	$\mathcal{D}(\widehat{R}, R)$	20	20	(0.5346,0.0807)	(0.2088,0.0550)	(0.7919,0.0888)	(0.7926,0.1480)
		20	100	(0.5101,0.0713)	(0.0664,0.0104)	(0.8091,0.0827)	(0.8215,0.1285)
		100	100	(0.5963,0.0496)	(0.0790,0.0054)	(0.9818,0.0087)	(0.9846,0.0071)
	$\mathcal{D}(\widehat{C}, C)$	20	20	(0.5237,0.0866)	(0.2159,0.0621)	(0.7968,0.0900)	(0.8047,0.1526)
		20	100	(0.1545,0.0213)	(0.1138,0.0104)	(0.8682,0.1089)	(0.9103,0.1168)
		100	100	(0.5968,0.0517)	(0.0793,0.0057)	(0.9805,0.0096)	(0.9842,0.0071)
skewed- t_3	$\mathcal{D}(\widehat{R}, R)$	20	20	(0.4707,0.1075)	(0.1824,0.0463)	(0.5657,0.1128)	(0.3681,0.2072)
		20	100	(0.5005,0.0788)	(0.0571,0.0085)	(0.5131,0.0912)	(0.1080,0.1760)
		100	100	(0.2795,0.1123)	(0.0654,0.0051)	(0.5980,0.1353)	(0.2816,0.2867)
	$\mathcal{D}(\widehat{C}, C)$	20	20	(0.4876,0.0992)	(0.1829,0.0434)	(0.5764,0.1058)	(0.3708,0.2084)
		20	100	(0.1192,0.0142)	(0.0962,0.0086)	(0.1985,0.1601)	(0.1552,0.1722)
		100	100	(0.2932,0.1161)	(0.0654,0.0044)	(0.5933,0.1300)	(0.2754,0.2843)

much more robustly under heavy-tailed and skewed noises, and as a result are more suitable for financial and econometrical applications.

5.3 Estimation Errors for Common Components

In this section, we compare the performances of of MPCA algorithms with those of $(2D)^2$ -PCA by [Zhang and Zhou \(2005\)](#) and PE method by [Yu et al. \(2021\)](#) in terms of estimating the common component matrices. We evaluate the performances by mean squared error (MSE) and maximum operator loss (opMax), which are defined as :

$$\text{MSE} = \frac{1}{Tpq} \sum_{t=1}^T \left\| \widehat{S}_t - S_t \right\|_F^2, \quad \text{opMax} = \frac{1}{(pq)^{1/2}} \max_{1 \leq t \leq T} \left\| \widehat{S}_t - S_t \right\|_{op},$$

where $\widehat{S}_t = P_{\widehat{R}} X_t P_{\widehat{C}}$ refers to the estimated common component matrix and S_t is the true value.

Table 2: Means and standard deviations (in parentheses) of MSE and opMax over 100 replications with $s_E = 1$ and $T = 3(pq)^{1/2}$. Here $MPCA_{op}$ and $MPCA_F$ stands for Manifold PCA methods; $(2D)^2$ -PCA is from [Zhang and Zhou \(2005\)](#), it is equivalent to α -PCA by [Chen and Fan \(2021\)](#) with $\alpha = -1$; PE stands for the projected estimation by [Yu et al. \(2021\)](#).

MSE						
Distribution	p	q	$MPCA_{op}$	$MPCA_F$	$(2D)^2$ -PCA	PE
Gauss	20	20	(0.0782,0.0222)	(0.0327,0.0030)	(0.0463,0.0141)	(0.0280,0.0024)
	20	100	(0.0277,0.0100)	(0.0031,0.0002)	(0.0052,0.0018)	(0.0026,0.0001)
	100	100	(0.0023,0.0005)	(0.0012,0.0000)	(0.0016,0.0003)	(0.0011,0.0000)
t_3	20	20	(0.2381,0.0299)	(0.1012,0.0158)	(0.3367,0.1668)	(0.2206,0.2185)
	20	100	(0.0405,0.0095)	(0.0086,0.0008)	(0.0767,0.2454)	(0.0466,0.2472)
	100	100	(0.0177,0.0068)	(0.0035,0.0002)	(0.0719,0.0947)	(0.0409,0.1010)
t_1	20	20	(46.248,271.94)	(42.431,252.56)	(1968.3,13474)	(1968.4,13474)
	20	100	(4.6400,37.238)	(4.0799,31.791)	(2180.1,19330)	(2180.1,19330)
	100	100	(0.8044,7.4323)	(0.7825,7.2180)	(888.12,7689.9)	(888.12,7689.9)
α -stable	20	20	(0.6030,0.9509)	(0.2638,0.3138)	(7.0910,29.585)	(7.1591,29.592)
	20	100	(0.0613,0.0313)	(0.0243,0.0288)	(1.9485,3.6707)	(1.9865,3.6689)
	100	100	(0.0698,0.0257)	(0.0113,0.0095)	(5.0615,9.6404)	(5.0704,9.6369)
skewed- t_3	20	20	(0.2273,0.0504)	(0.0979,0.0232)	(0.3977,0.2926)	(0.2918,0.3304)
	20	100	(0.0397,0.0089)	(0.0085,0.0007)	(0.0747,0.1179)	(0.0442,0.1293)
	100	100	(0.0160,0.0068)	(0.0035,0.0001)	(0.0797,0.0671)	(0.0519,0.0789)
opMax						
Distribution	p	q	$MPCA_{op}$	$MPCA_F$	$(2D)^2$ -PCA	PE
Gauss	20	20	(0.0820,0.0207)	(0.0501,0.0047)	(0.0600,0.0132)	(0.0490,0.0047)
	20	100	(0.0487,0.0112)	(0.0104,0.0007)	(0.0158,0.0045)	(0.0101,0.0008)
	100	100	(0.0067,0.0011)	(0.0047,0.0003)	(0.0053,0.0006)	(0.0047,0.0003)
t_3	20	20	(0.1554,0.0377)	(0.1166,0.0398)	(0.3523,0.2749)	(0.3187,0.3208)
	20	100	(0.0558,0.0145)	(0.0252,0.0148)	(0.1291,0.2865)	(0.0927,0.2944)
	100	100	(0.0216,0.0061)	(0.0116,0.0075)	(0.1516,0.2322)	(0.1239,0.2463)
t_1	20	20	(3.2655,11.248)	(3.1082,10.779)	(21.583,73.268)	(21.583,73.268)
	20	100	(0.8514,3.6067)	(0.8207,3.3761)	(16.575,78.617)	(16.575,78.617)
	100	100	(0.3369,1.5060)	(0.3332,1.4852)	(12.686,49.611)	(12.687,49.611)
α -stable	20	20	(0.5956,0.6924)	(0.4152,0.4161)	(2.4968,3.4367)	(2.5217,3.4254)
	20	100	(0.1406,0.1292)	(0.1192,0.1212)	(1.5301,1.4189)	(1.5386,1.4144)
	100	100	(0.1327,0.1149)	(0.0792,0.0668)	(2.5643,2.2154)	(2.5652,2.2148)
skewed- t_3	20	20	(0.1754,0.0943)	(0.1363,0.0750)	(0.4477,0.3798)	(0.4439,0.4152)
	20	100	(0.0557,0.0158)	(0.0271,0.0136)	(0.1470,0.2371)	(0.1112,0.2496)
	100	100	(0.0199,0.0058)	(0.0116,0.0035)	(0.1986,0.2064)	(0.1684,0.2300)

Table 2 reports the means and standard deviations of MSEs and opMaxs with $s_E = 1$. Simulation results with $s_E \in \{1.5, 2\}$ are reported in Table 8 and 9 in the supplementary materials. Similar as the conclusions drawn for factor loadings, both $MPCA_F$ and PE also benefit from the projection effect. MPCA methods are comparable with $(2D)^2$ -PCA and PE under light-tailed noises, but are much more robust under the heavy-tailed and skewed noises.

5.4 Estimation of Factor Numbers

Accurate estimation of the pair of factor numbers is of vital importance in matrix factor analysis. In this section, we compare the empirical performances of our MER_{op} , MER_F algorithms with IterER

method by Yu et al. (2021) and $(2D)^2$ -ER method, which is equivalent to the eigenvalue-ratio method in Chen and Fan (2021) with $\alpha = -1$.

Table 3: Frequencies of exact estimation and underestimation (in parentheses) of factor numbers over 100 replications with $s_E = 1$ and $T = 3(pq)^{1/2}$. Here MER_{op} and MER_F stands for Manifold eigenvalue-ratio methods; $(2D)^2$ -ER is equivalent to the ER method in Chen and Fan (2021) with $\alpha = -1$; IterER is from Yu et al. (2021).

Distribution	p	q	MER_{op}	MER_F	$(2D)^2$ -ER	IterER
Gaussian	20	20	(0.37,0.19)	(0.95,0.04)	(0.12,0.73)	(0.94,0.06)
	20	100	(0.98,0.00)	(1.00,0.00)	(0.19,0.37)	(1.00,0.00)
	100	100	(1.00,0.00)	(1.00,0.00)	(0.36,0.00)	(1.00,0.00)
t_3	20	20	(0.13,0.65)	(0.53,0.43)	(0.04,0.83)	(0.33,0.63)
	20	100	(0.17,0.13)	(1.00,0.00)	(0.05,0.50)	(0.80,0.02)
	100	100	(0.04,0.02)	(1.00,0.00)	(0.00,0.24)	(0.51,0.03)
t_1	20	20	(0.99,0.01)	(1.00,0.00)	(0.02,0.85)	(0.01,0.76)
	20	100	(1.00,0.00)	(1.00,0.00)	(0.08,0.82)	(0.08,0.72)
	100	100	(1.00,0.00)	(1.00,0.00)	(0.07,0.86)	(0.05,0.88)
α -stable	20	20	(0.05,0.85)	(0.37,0.63)	(0.02,0.95)	(0.01,0.94)
	20	100	(0.26,0.47)	(1.00,0.00)	(0.03,0.92)	(0.04,0.85)
	100	100	(0.06,0.93)	(0.95,0.05)	(0.07,0.87)	(0.07,0.91)
skewed- t_3	20	20	(0.08,0.83)	(0.61,0.38)	(0.03,0.91)	(0.33,0.59)
	20	100	(0.23,0.12)	(1.00,0.00)	(0.16,0.47)	(0.75,0.03)
	100	100	(0.07,0.06)	(1.00,0.00)	(0.00,0.37)	(0.43,0.02)

Table 3 reports the frequencies of exact estimation and underestimation with $s_E = 1$. Simulation results with $s_E \in \{1.5, 2\}$ are reported in Table 10 and Table 11 in the supplementary materials. We set $r_{\max} = 8$ for all the algorithms. It is observed that both MER_F and IterER benefit from the projection effect. In addition, MER_F is no worse than IterER for Gaussian noise, and outperforms IterER by a large margin for the heavy-tailed and skewed noises. As a result, MER_F can be used as a safe replacement of IterER in financial and econometrical applications.

6 Real Data Analysis

In this section, we apply the proposed algorithms on a financial portfolio dataset as in Wang et al. (2019), Yu et al. (2021). The dataset consists of monthly returns of 100 portfolios from January 1964 to December 2019, covering 672 months. The portfolios are constructed into 10×10 data matrices, whose rows correspond to market capital size (S1-S10), and columns correspond to book-to-equity ratio (BE1-BE10). Detailed information could be found on the website http://mba.tuck.dartmouth.edu/pages/faculty/ken.french/data_library.html.

Following Wang et al. (2019) and Yu et al. (2021), we first subtract the corresponding monthly excess returns and impute the missing data by linear interpolation. The augmented Dickey-Fuller tests indicate stationarity of all time series. We apply eigenvalue-ratio algorithms on the full dataset to determine the pair of factor numbers p_0 and q_0 , where MER_{op} , $(2D)^2$ -ER suggest $p_0 = q_0 = 1$, while MER_F , IterER

suggest $p_0 = 1$ and $q_0 = 2$. As the latter two projected algorithms are more stable under moderate noise shown in simulation study, we take $p_0 = 1$ and $q_0 = 2$ for further analysis.

Table 4: Factor loadings with $p_0 = 1$ and $q_0 = 2$ for Fama-French dataset after varimax rotation and scaling by 30. Here $MPCA_F$ and $MPCA_{op}$ stands for Manifold PCA methods; PE stands for the projected estimation by Yu et al. (2021); $(2D)^2$ -PCA is from Zhang and Zhou (2005), it is equivalent to α -PCA by Chen and Fan (2021) with $\alpha = -1$.

Size											
Method	Factor	S1	S2	S3	S4	S5	S6	S7	S8	S9	S10
$MPCA_{op}$	1	-10	-10	-11	-11	-11	-11	-9	-9	-6	0
$MPCA_F$	1	-11	-12	-12	-11	-11	-10	-9	-8	-5	0
$(2D)^2$ -PCA	1	-10	-11	-12	-11	-11	-10	-9	-8	-6	0
PE	1	-11	-12	-12	-11	-11	-10	-8	-7	-5	0
Book-to Equity											
Method	Factor	BE1	BE2	BE3	BE4	BE5	BE6	BE7	BE8	BE9	BE10
$MPCA_{op}$	1	3	0	-4	-6	-10	-11	-13	-12	-12	-12
	2	17	18	13	9	4	2	-1	-1	-3	-3
$MPCA_F$	1	3	0	-4	-6	-9	-11	-12	-13	-13	-12
	2	19	17	11	8	5	1	-1	-2	-3	-3
$(2D)^2$ -PCA	1	3	-1	-5	-8	-10	-12	-12	-12	-12	-11
	2	19	18	12	7	3	0	-2	-3	-2	-2
PE	1	3	-2	-5	-8	-10	-11	-12	-12	-13	-11
	2	21	16	11	7	3	0	-2	-3	-2	-1

The estimated loading matrices after varimax rotation and scaling are reported in Table 4. It is observed that $MPCA_{op}$, $MPCA_F$, $(2D)^2$ -PCA and PE methods lead to similar estimated loadings. The small size portfolios load heavily on the front loading. The two factors in the back loading separate portfolios well from the perspective of book-to-equity, with large BE portfolios loading mainly on the first factor, and small BE portfolios loading mainly on the second.

Figure 2 shows the time series plots of the 100 series, while Figure 3 shows the estimated factors by $MPCA_{op}$ and $MPCA_F$ with $p_0 = 1$ and $q_0 = 2$, which show similar patterns and further indicate the estimated factors could potentially replace the original data matrices for further analysis.

To further compare these methods, we apply similar rolling-validation procedures as in Wang et al. (2019) and Yu et al. (2021). For each year t from 1996 to 2019, we take n (bandwidth) years before t as the training set, which is used to fit matrix factor models. The estimated loadings are then used to estimate factors and corresponding residuals of the testing set, consisting of the 12 months next year. Specifically, let Y_t^i and \hat{Y}_t^i be the observed and predicted price matrix of month i in year t , we focus on the errors MSE_t and $opMax_t$ defined as:

$$MSE_t = \frac{1}{12 \times 10 \times 10} \sum_{i=1}^{12} \left\| Y_t^i - \hat{Y}_t^i \right\|_F^2, \quad opMax_t = \frac{1}{10} \max_{1 \leq i \leq 12} \left\| Y_t^i - \hat{Y}_t^i \right\|_{op}.$$

Table 5 reports the means and standard deviations of MSE_t and $opMax_t$ by $MPCA_{op}$, $MPCA_F$, $(2D)^2$ -PCA and PE methods. The reported errors of different methods are very close, but $MPCA_F$ performs slightly better under almost all bandwidths n , in terms of both MSE_t and $opMax_t$. Financial

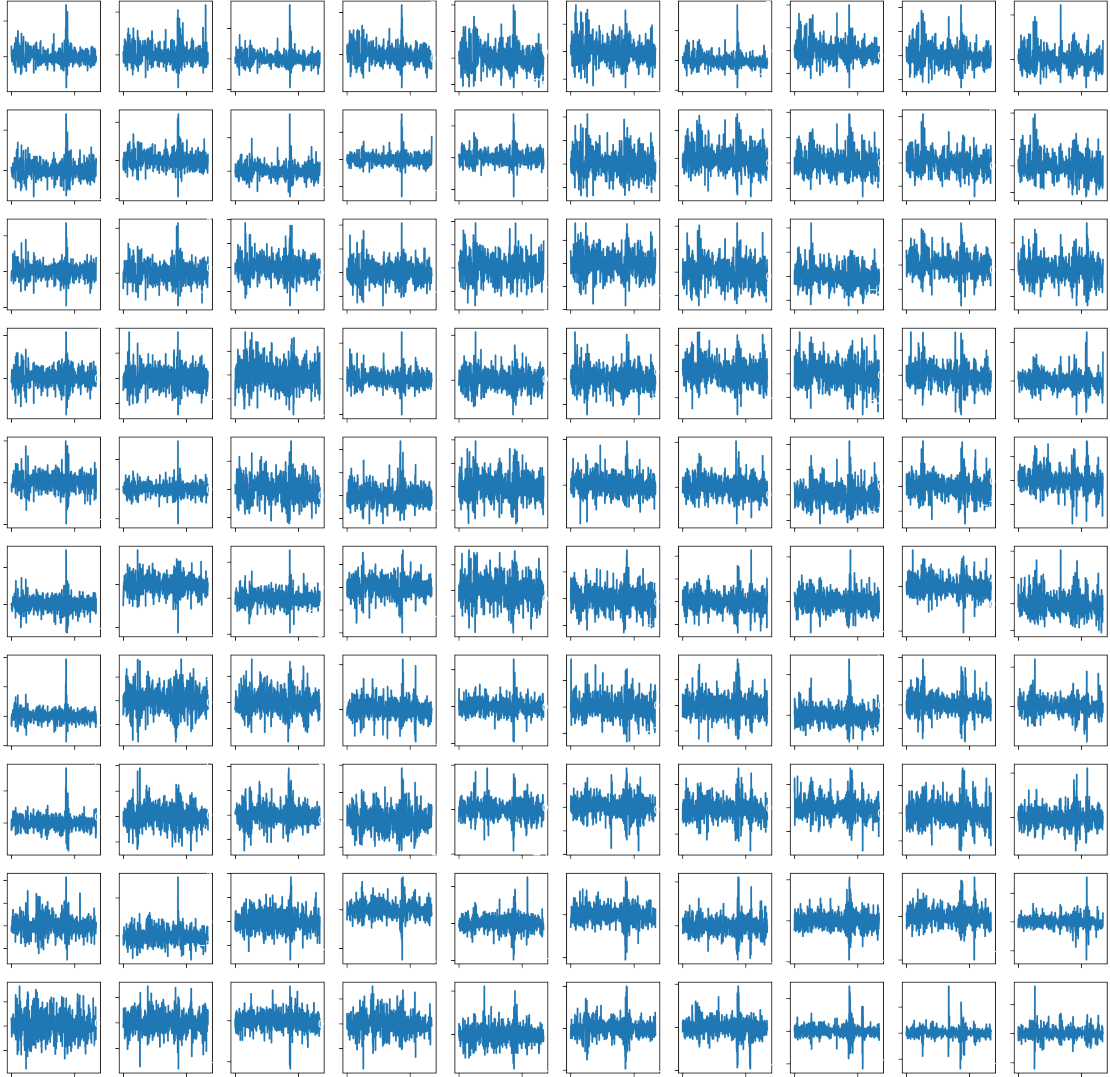


Figure 2: Time series plots of Fama-French 10 by 10 series.

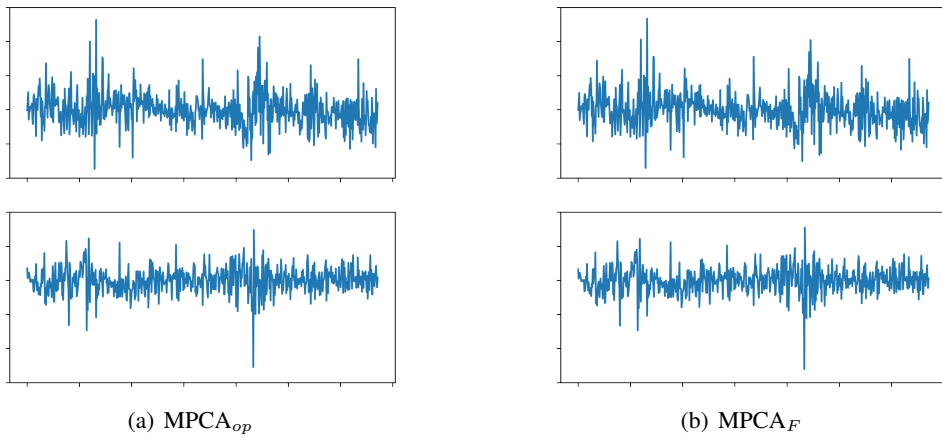


Figure 3: Plots of \hat{F}_t estimated by $MPCA_{op}$ and $MPCA_F$ respectively after varimax rotation.

Table 5: Rolling validation with $p_0 = 1$ and $q_0 = 2$ for Fama-French dataset, the sample size of training set is $12n$. We report the means and standard deviations (in parentheses) of MSE_t and opMax_t . Here MPCA_F and MPCA_{op} stands for Manifold PCA methods; PE stands for the projected estimation by Yu et al. (2021); $(2D)^2$ -PCA is from Zhang and Zhou (2005), which is equivalent to α -PCA by Chen and Fan (2021) with $\alpha = -1$.

MSE				
n	MPCA_{op}	MPCA_F	$(2D)^2$ -PCA	PE
5	(0.7423,0.7372)	(0.7405,0.7490)	(0.7410,0.7291)	(0.7378,0.7310)
10	(0.7430,0.7413)	(0.7431,0.7544)	(0.7512,0.7377)	(0.7472,0.7431)
15	(0.7488,0.7568)	(0.7456,0.7637)	(0.7524,0.7525)	(0.7470,0.7529)
20	(0.7452,0.7528)	(0.7417,0.7578)	(0.7499,0.7534)	(0.7451,0.7534)
25	(0.7444,0.7501)	(0.7407,0.7559)	(0.7492,0.7574)	(0.7450,0.7566)
opMax				
n	MPCA_{op}	MPCA_F	$(2D)^2$ -PCA	PE
5	(0.7599,0.4774)	(0.7509,0.4714)	(0.7568,0.4764)	(0.7509,0.4708)
10	(0.7600,0.4784)	(0.7482,0.4694)	(0.7683,0.4660)	(0.7538,0.4591)
15	(0.7597,0.4768)	(0.7482,0.4654)	(0.7647,0.4655)	(0.7515,0.4564)
20	(0.7621,0.4839)	(0.7497,0.4726)	(0.7666,0.4701)	(0.7528,0.4600)
25	(0.7627,0.4788)	(0.7488,0.4682)	(0.7625,0.4626)	(0.7493,0.4557)

data is well-known to be heavy-tailed, and thus the more robust MPCA_F is always preferred.

7 Conclusions and Discussions

Data in real world such as financial returns are well-known to be heavy-tailed, and robust factor modelling is indispensable as the traditional PCA estimation method would result in bigger biases and higher dispersions as the distribution tails become heavier (He et al., 2022, 2021b). In this article, we for the first time propose a flexible Matrix Elliptical Factor Model (MEFM) for better modelling heavy-tailed matrix-valued data, which can be viewed as an extension of the matrix factor model by Wang et al. (2019). We also propose robust Manifold Principle Component Analysis (MPCA) procedures to estimate the factor loading, scores, and common components matrices without any moment constraint under the framework of Matrix Elliptical Distributions (MED). We explore two versions of MPCA algorithms, denoted as MPCA_F and MPCA_{op} , by considering the optimization problems in (2.2) under matrix operator norm and matrix frobenius norm respectively. Theoretical convergence rates of the estimators are derived for both versions. However, the MPCA_F method is not only robust to heavy-tailed data, but also enjoys the nice property of the projection technique, thus performs the best in finite-sample experiments. In addition, we also proposed two robust versions to estimate the pair of factor numbers, by calculating eigenvalue-ratios (ER) of the average projection matrices corresponding to MPCA_F and MPCA_{op} . We prove that the estimators of the pair of factor numbers are consistent. We conduct extensive numerical studies to validate the empirical performance of the proposed robust methods and an application to a Fama-French financial portfolios dataset illustrates the practical value of the current work. In the theoretical analysis of the MPCA_F , we assume that either R or C is given

to establish the convergence rate of C or R , which is not quite satisfying. As a future work, we will establish the convergence rates of estimators from the iterative procedure, which is more challenging as both statistical error and computational error should be taken into account.

Acknowledgements

He's work is supported by National Science Foundation (NSF) of China (12171282,11801316), National Statistical Scientific Research Key Project (2021LZ09), Young Scholars Program of Shandong University, Project funded by China Postdoctoral Science Foundation (2021M701997) and the Fundamental Research Funds of Shandong University. Kong's work is partially supported by NSF China (71971118 and 11831008) and the WRJH-QNBJ Project and Qinglan Project of Jiangsu Province. Zhang's work is supported by NSF China (11971116).

References

- Ahn, S.C., Horenstein, A.R., 2013. Eigenvalue ratio test for the number of factors. *Econometrica* 81, 1203–1227.
- Bai, J., 2003. Inferential theory for factor models of large dimensions. *Econometrica* 71, 135–171.
- Bai, J., Li, K., 2012. Statistical analysis of factor models of high dimension. *The Annals of Statistics* 40, 436–465.
- Bai, J., Li, K., 2016. Maximum likelihood estimation and inference for approximate factor models of high dimension. *Review of Economics and Statistics* 98, 298–309.
- Bai, J., Ng, S., 2002. Determining the number of factors in approximate factor models. *Econometrica* 70, 191–221.
- Chen, E.Y., Fan, J., 2021. Statistical inference for high-dimensional matrix-variate factor models. *Journal of the American Statistical Association*, 1–18.
- Chen, L., Dolado, J.J., Gonzalo, J., 2021a. Quantile factor models. *Econometrica* 89, 875–910.
- Chen, Y., Chi, Y., Fan, J., Ma, C., et al., 2021b. Spectral methods for data science: A statistical perspective. *Foundations and Trends® in Machine Learning* 14, 566–806.
- Edelman, A., 1988. Eigenvalues and condition numbers of random matrices. *SIAM journal on matrix analysis and applications* 9, 543–560.
- Fan, J., Liao, Y., Mincheva, M., 2013. Large covariance estimation by thresholding principal orthogonal complements. *Journal of the Royal Statistical Society: Series B (Statistical Methodology)* 75, 603–680.
- Fan, J., Liu, H., Wang, W., 2018. Large covariance estimation through elliptical factor models. *The Annals of Statistics: An Official Journal of the Institute of Mathematical Statistics* 46, 1383–1414.

- Gupta, A., Varga, T., 1994. A new class of matrix variate elliptically contoured distributions. *Journal of the Italian Statistical Society* 3, 255–270.
- Gupta, A.K., Nagar, D.K., 2018. *Matrix variate distributions*. volume 104. CRC Press.
- Ham, J., Lee, D.D., 2008. Grassmann discriminant analysis: a unifying view on subspace-based learning, in: *Machine Learning, Twenty-fifth International Conference, Helsinki, Finland, June*.
- He, Y., Kong, X., Trapani, L., Yu, L., 2021a. Vector factor model or matrix factor model? A strong rule helps! *arXiv: arXiv:2110.01008* .
- He, Y., Kong, X., Yu, L., Zhang, P., 2020. Learning quantile factors for large-dimensional time series with statistical guarantee. *arXiv:2006.08214* .
- He, Y., Kong, X., Yu, L., Zhang, X., 2022. Large-dimensional factor analysis without moment constraints. *Journal of Business & Economic Statistics* 40, 302–312.
- He, Y., Kong, X., Yu, L., Zhang, X., Zhao, C., 2021b. Statistical inference for large-dimensional matrix factor model from least squares and huber loss points of view. *arXiv:2112.04186* .
- He, Y., Kong, X.B., Trapani, L., Yu, L., 2021c. Online change-point detection for matrix-valued time series with latent two-way factor structure. *arXiv:2112.13479* .
- Onatski, A., 2009. Testing hypotheses about the number of factors in large factor models. *Econometrica* 77, 1447–1479.
- Ross, S.A., 1976. The arbitrage theory of capital asset pricing. *Journal of Finance* 13, 341–360.
- Rudelson, M., Vershynin, R., 2010. Non-asymptotic theory of random matrices: extreme singular values, in: *Proceedings of the International Congress of Mathematicians 2010 (ICM 2010) (In 4 Volumes) Vol. I: Plenary Lectures and Ceremonies Vols. II–IV: Invited Lectures*, World Scientific. pp. 1576–1602.
- Stock, J.H., Watson, M.W., 2002. Forecasting using principal components from a large number of predictors. *Journal of the American statistical association* 97, 1167–1179.
- Trapani, L., 2018. A randomised sequential procedure to determine the number of factors. *Journal of the American Statistical Association* 113, 1341–1349.
- Tropp, J.A., 2012. User-friendly tail bounds for sums of random matrices. *Foundations of computational mathematics* 12, 389–434.
- Tropp, J.A., 2015. An introduction to matrix concentration inequalities. *arXiv preprint arXiv:1501.01571* .
- Wang, D., Liu, X., Chen, R., 2019. Factor models for matrix-valued high-dimensional time series. *Journal of econometrics* 208, 231–248.

- Yu, L., He, Y., Kong, X., Zhang, X., 2021. Projected estimation for large-dimensional matrix factor models. *Journal of Econometrics*, in press. doi:[10.1016/j.jeconom.2021.04.001](https://doi.org/10.1016/j.jeconom.2021.04.001).
- Yu, L., He, Y., Zhang, X., 2019. Robust factor number specification for large-dimensional elliptical factor model. *Journal of Multivariate analysis* 174, 104543.
- Yu, Y., Wang, T., Samworth, R.J., 2015. A useful variant of the davis–kahan theorem for statisticians. *Biometrika* 102, 315–323.
- Zhang, D., Zhou, Z.H., 2005. (2d) 2pca: Two-directional two-dimensional pca for efficient face representation and recognition. *Neurocomputing* 69, 224–231.

Supplementary Materials for “Manifold Principle Component Analysis for Large-Dimensional Matrix Elliptical Factor Model”

ZeYu Li^{* §}, Yong He^{† §}, Xinbing Kong[‡], Xinsheng Zhang^{*}

This document provides detailed proofs and additional simulation results of the main paper.

A Proof of Lemma 3.1

It is a direct consequence of the matrix Hoeffding inequality from Tropp (2012), we only need to verify that $[P_{\widehat{R}_t} - \mathbb{E}P_{\widehat{R}_t}]^2 \preceq I_p$ almost surely. Since $0 \leq \langle v, P_{\widehat{R}_t} v \rangle \leq 1$ almost surely and thus $0 \leq \langle v, \mathbb{E}P_{\widehat{R}_t} v \rangle \leq 1$ for all $\|v\|_2 = 1$, we have $\|P_{\widehat{R}_t} - \mathbb{E}P_{\widehat{R}_t}\|_{op} \leq 1$ almost surely. The rest would be straightforward.

B Proof of Lemma 3.2

For joint matrix elliptical data $X_t = RF_t C^\top + E_t$, since E_t is left spherical, we could write $F_t = r_t \Sigma_1^{1/2} Z_t^F \Sigma_2^{1/2} / \|Z_t\|_2$ and $E_t = r_t Z_t^E \Omega_2^{1/2} / \|Z_t\|_2$ under model 2.1. Let $Z_t^{\prime E} = (2P_R - I)Z_t^E$, then $\|Z_t\|_2^2 = \|Z_t^F\|_F^2 + \|Z_t^E\|_F^2 = \|Z_t^F\|_F^2 + \|Z_t^{\prime E}\|_F^2 = \|Z_t'\|_2^2$ almost surely, where Z_t' is defined as $(\text{Vec}(Z_t^F)^\top, \text{Vec}(Z_t^{\prime E})^\top)$. Due to rotational invariance of Z_t^E , Z_t is identically distributed to Z_t' , the latter generates $X_t' = RF_t' C^\top + E_t' \stackrel{d}{=} X_t$. Now that $F_t' = r_t \Sigma_1^{1/2} Z_t^F \Sigma_2^{1/2} / \|Z_t'\|_2 = F_t$ almost surely, while $E_t' = r_t Z_t^{\prime E} \Omega_2^{1/2} / \|Z_t'\|_2 = (2P_R - I)E_t$ almost surely, we have $X_t' = (2P_R - I)X_t$ almost surely. Since X_t and X_t' are identically distributed, so do their best linear subspace estimations \widehat{R}_t and \widehat{R}_t' , so that:

$$\mathbb{E} [P_{\widehat{R}_t}] = \mathbb{E} [P_{\widehat{R}_t} + P_{\widehat{R}_t'}] / 2.$$

From $X_t' = (2P_R - I)X_t$ we know that the column vectors of X_t' and X_t are symmetric in respect of $\text{Span}(R)$, so should their leading left singular vectors \widehat{R}_t' and \widehat{R}_t , which gives $P_{\widehat{R}_t'} = (2P_R - I)P_{\widehat{R}_t}(2P_R - I)$. That is to say, $\forall u \in \text{Span}(R)$, $(P_{\widehat{R}_t} + P_{\widehat{R}_t'})u = 2P_R P_{\widehat{R}_t} u \in \text{Span}(R)$. Similarly, $\forall v \in \text{Span}(R^\perp)$, $(P_{\widehat{R}_t} + P_{\widehat{R}_t'})v = 2(I - P_R)P_{\widehat{R}_t} v \in \text{Span}(R^\perp)$. In the end, since \mathbb{E} is linear, $\mathbb{E} [P_{\widehat{R}_t} + P_{\widehat{R}_t'}] u \in \text{Span}(R)$ and $\mathbb{E} [P_{\widehat{R}_t} + P_{\widehat{R}_t'}] v \in \text{Span}(R^\perp)$, we claim the proof.

C Proof of Theorem 3.3

Without loss of generality, we only prove $\text{Span}(R)$ here. For notation simplicity, here we let \widehat{R} to be the result from MPCA_{op} , instead of \widehat{R}_{op} . Before the proof, recall a well-known fact that for $P_{\widehat{R}} = \widehat{R}\widehat{R}^\top / p$ and $P_R = RR^\top / p$:

$$\|P_{\widehat{R}} - P_R\|_F^2 \asymp \min_{H_R \in \mathcal{O}_{p_0, p_0}} \|\widehat{R} - RH_R\|_F^2 / p,$$

^{*}Department of Statistics, School of Management at Fudan University, China; e-mail:zeyuli21@m.fudan.edu.cn; xszhang@fudan.edu.cn

[†]Institute of Financial Studies, Shandong University, China; e-mail:heyong@sdu.edu.cn

[‡]Nanjing Audit University, China; e-mail:xinbingkong@126.com

[§]The authors contributed equally to this work.

where the left hand side is known as the projection metric on Grassmann manifolds. So it is equivalent to study the term $\|P_{\hat{R}} - P_R\|_F$ instead, see [Chen et al. \(2021b\)](#) for details.

C.1 Spherical Neighbour

From lemma 3.2, it is ideal if E_t is left spherical when estimating $\text{Span}(R)$, right spherical when estimating $\text{Span}(C)$, and spherical when estimating both. Unfortunately, let $\zeta_t = r_t/\|Z_t\|_2$, the noise $E_t = \zeta_t \Omega_1^{1/2} Z_t^E \Omega_2^{1/2}$ is elliptically transformed by Ω_1 and Ω_2 . It is then natural to evaluate how much harm would deviating to non-spherical noise do. A spherical neighbour argument is applied where we construct a desirable \dot{E}_t sufficiently close to E_t , controlling the difference by matrix perturbation results. Since we are currently dealing with $\text{Span}(R)$, \dot{E}_t needs to be left spherical. Let $\omega_1 = \arg \min_{\omega} \|\Omega_1^{1/2} - \omega^{1/2} I_p\|_{op}$, define $\dot{E}_t = \zeta_t \omega_1^{1/2} Z_t^E \Omega_2^{1/2}$. Denote $\dot{X}_t = RF_t C^\top + \dot{E}_t$, $\dot{P}_{\hat{R}_t}$ as the empirical projection matrix from each \dot{X}_t , and $\dot{P}_{\hat{R}}$ as the MPCA_{op} result from $\{\dot{X}_t\}$, then by triangular inequality we have:

$$\|P_{\hat{R}} - P_R\|_F \leq \|P_{\hat{R}} - \dot{P}_{\hat{R}}\|_F + \|\dot{P}_{\hat{R}} - P_R\|_F. \quad (\text{C.1})$$

We first focus on the term $\|P_{\hat{R}} - \dot{P}_{\hat{R}}\|_F$, which comes from noise E_t being non-spherical. Define $d_i(A) = (\lambda_i - \lambda_{i+1})(A)$ as the i -th eigengap of matrix A , where λ_i is the i -th non-increasing eigenvalue of A . Consider the matrix perturbation $\sum_{t=1}^T P_{\hat{R}_t}/T = \sum_{t=1}^T \dot{P}_{\hat{R}_t}/T + \sum_{t=1}^T (P_{\hat{R}_t} - \dot{P}_{\hat{R}_t})/T$, by YWS's inequality from [Yu et al. \(2015\)](#) and Jensen's inequality:

$$\|P_{\hat{R}} - \dot{P}_{\hat{R}}\|_F \leq \frac{2\sqrt{2} \|\sum_{t=1}^T (P_{\hat{R}_t} - \dot{P}_{\hat{R}_t})/T\|_F}{d_{p_0}(\sum_{t=1}^T \dot{P}_{\hat{R}_t}/T)} \leq \frac{2\sqrt{2} \sum_{t=1}^T \|P_{\hat{R}_t} - \dot{P}_{\hat{R}_t}\|_F}{T d_{p_0}(\sum_{t=1}^T \dot{P}_{\hat{R}_t}/T)}. \quad (\text{C.2})$$

We are going to show that $d_{p_0}(\mathbb{E} \dot{P}_{\hat{R}_t}) > 0$ and $\|\sum_{t=1}^T \dot{P}_{\hat{R}_t}/T - \mathbb{E} \dot{P}_{\hat{R}_t}\|_{op} \rightarrow 0$ as $T, p, q \rightarrow \infty$ in later analysis. By Weyl's inequality the eigengap $d_{p_0}(\sum_{t=1}^T \dot{P}_{\hat{R}_t}/T) \rightarrow d_{p_0}(\mathbb{E} \dot{P}_{\hat{R}_t}) > 0$. So we focus on the term $\sum_{t=1}^T \|P_{\hat{R}_t} - \dot{P}_{\hat{R}_t}\|_F/T$. Consider the perturbation $X_t = \dot{X}_t + (E_t - \dot{E}_t)$, by Wedin's theorem and Weyl's inequality:

$$\|P_{\hat{R}_t} - \dot{P}_{\hat{R}_t}\|_F \leq \frac{2\sqrt{r_0} \|E_t - \dot{E}_t\|_{op}}{\sigma_{t,r_0} - 2\|\dot{E}_t\|_{op} - \|E_t - \dot{E}_t\|_{op}} \wedge \sqrt{2r_0}, \quad (\text{C.3})$$

where σ_{t,r_0} is the r_0 -th singular value of the signal part $S_t = RF_t C^\top$, and by sub-multiplicativity of operator norm:

$$\|E_t - \dot{E}_t\|_{op} = \frac{\|(\Omega_1^{1/2} - \omega_1^{1/2} I_p) \dot{E}_t\|_{op}}{\omega_1^{1/2}} \leq \frac{\|\Omega_1^{1/2} - \omega_1^{1/2} I_p\|_{op}}{\omega_1^{1/2}} \|\dot{E}_t\|_{op}. \quad (\text{C.4})$$

Then under Assumption A to C, we have

$$\mathbb{E} \|P_{\hat{R}_t} - \dot{P}_{\hat{R}_t}\|_F = O(p^{-1/4} + q^{-1/4}). \quad (\text{C.5})$$

Intuitively, under strong factor model, $\sigma_{t,r_0} \gtrsim (pq)^{1/2} \zeta_t \sigma_{r_0}(Z_t^F)$ and $\|\dot{E}_t\|_{op} \lesssim (p \vee q)^{1/2} \zeta_t$, so that $\mathbb{E} \|P_{\hat{R}_t} - \dot{P}_{\hat{R}_t}\|_F$ tends to zero as $p, q \rightarrow \infty$ from C.3 and C.4. To be more specific, here without loss of generality assume $p_0 = r_0 \leq q_0$, consider the matrix $S_t S_t^\top = qRF_t F_t^\top R^\top$, whose r_0 -th eigenvalue

is σ_{t,r_0}^2 . Let $v = Ru/\sqrt{p}$, $\|u\|_2 = 1$ be the unit vector of r_0 -dimensional subspace $\text{Span}(R)$, then $\langle v, S_t S_t^\top v \rangle = pq \langle u, F_t F_t^\top u \rangle \geq pq \sigma_{r_0}^2(F_t) \geq pq(c_1 \zeta_t)^2 \sigma_{r_0}^2(Z_t^F)$, $\forall v \in \text{Span}(R)$, the last inequality comes from $\|\Sigma_1^{1/2} Z_t^F \Sigma_2^{1/2} w\|_2 \geq c_1 \sigma_{r_0}(Z_t^F)$ for all $\|w\|_2 = 1$. By Courant–Fischer’s minimax theorem, $\sigma_{t,r_0} \geq (pq)^{1/2} c_1 \zeta_t \sigma_{r_0}(Z_t^F)$, while $\|\dot{E}_t\|_{op} \lesssim \zeta_t \|Z_t^E\|_{op}$ is straightforward by sub-multiplicativity of operator norm. Consider the ratio in C.3, under joint matrix elliptical model in Assumption A, the shared ζ_t is cancelled out, we only need to focus on the expectation of $(pq)^{-1/2} \|Z_t^E\|_{op} / \sigma_{r_0}(Z_t^F)$, whose numerator and denominator are independent.

Non-asymptotic random matrix theory asserts that $\sigma_{r_0}(Z_t^F) \asymp \sqrt{q_0} - \sqrt{p_0}$, so $\mathbb{E}\|P_{\hat{R}_t} - \dot{P}_{\hat{R}_t}\|_F = O(p^{-1/2} + q^{-1/2})$ unless $p_0 = q_0 = r_0$, only then $\sigma_{r_0}(Z_t^F)$ has a larger probability towards 0, leading to invertibility problems. In this case, we could use the fact from Edelman (1988) that:

$$\mathbb{P}\left(\sigma_{r_0}(Z_t^F) \leq \varepsilon r_0^{-1/2}\right) \leq \varepsilon, \quad \forall \varepsilon \geq 0,$$

see Rudelson and Vershynin (2010) for details on extreme singular values of random matrices. If $p \geq q$, let $\varepsilon = q^{-1/4}$, and $\mathbb{P}\left(\sigma_{r_0}(Z_t^F) \leq q^{-1/4}\right) \lesssim q^{-1/4}$. Then we have:

$$\begin{aligned} \mathbb{E}\|P_{\hat{R}_t} - \dot{P}_{\hat{R}_t}\|_F &= \mathbb{E}\left(\|P_{\hat{R}_t} - \dot{P}_{\hat{R}_t}\|_F I_{\{\sigma_{r_0}(Z_t^F) \leq q^{-1/4}\}}\right) \\ &\quad + \mathbb{E}\left(\|P_{\hat{R}_t} - \dot{P}_{\hat{R}_t}\|_F I_{\{\sigma_{r_0}(Z_t^F) > q^{-1/4}\}}\right) \\ &\lesssim \sqrt{2r_0} \mathbb{P}\left(\sigma_{r_0}(Z_t^F) \leq q^{-1/4}\right) + q^{-1/4} = O(q^{-1/4}), \end{aligned} \quad (\text{C.6})$$

where $\mathbb{E}(\|P_{\hat{R}_t} - \dot{P}_{\hat{R}_t}\|_F I_{\{\sigma_{r_0}(Z_t^F) > q^{-1/4}\}}) \lesssim q^{-1/4}$ comes from the fact that when $\sigma_{r_0}(Z_t^F) > q^{-1/4}$, we have $\sigma_{t,r_0} \geq c_1 \zeta_t p^{1/2} q^{1/4}$, and $\|P_{\hat{R}_t} - \dot{P}_{\hat{R}_t}\|_F \lesssim \|\dot{E}_t\|_{op} / \sigma_{t,r_0} \lesssim q^{-1/4}$ from C.3. Similarly, if $p < q$, $\mathbb{E}\|P_{\hat{R}_t} - \dot{P}_{\hat{R}_t}\|_F = O(p^{-1/4})$. In the end, since $\|P_{\hat{R}_t} - \dot{P}_{\hat{R}_t}\|_F \leq \sqrt{2r_0}$ almost surely, apply scalar concentration to C.2, C.5 and:

$$\|P_{\hat{R}} - \dot{P}_{\hat{R}}\|_F \lesssim \frac{\sum_{t=1}^T \|P_{\hat{R}_t} - \dot{P}_{\hat{R}_t}\|_F}{T} = O_p(T^{-1/2} + p^{-1/4} + q^{-1/4}), \quad (\text{C.7})$$

that is to say, the influence of E_t being non-spherical is ignorable as $T, p, q \rightarrow \infty$.

We then focus on the second term $\|\dot{P}_{\hat{R}} - P_R\|_F$ in C.1, the convergence of MPCA_{op} under spherical noise \dot{E}_t . With slight abuse of notation but no loss of generality, the model could be reset as $X_t = RF_t C^\top + E_t$, where $\Omega_1 = \omega_1 I_p$ and E_t is left spherical. The second term is then $\|P_{\hat{R}} - P_R\|_F$. Since $\text{Span}(R)$ is the invariant subspace of $\mathbb{E}P_{\hat{R}_t}$ according to lemma 3.2, consider the matrix perturbation $\sum_{t=1}^T P_{\hat{R}_t} / T = \mathbb{E}P_{\hat{R}_t} + (\sum_{t=1}^T P_{\hat{R}_t} / T - \mathbb{E}P_{\hat{R}_t})$, by YWS’s inequality we have:

$$\|P_{\hat{R}} - P_R\|_F \leq \frac{2\sqrt{2p_0} \|\sum_{t=1}^T P_{\hat{R}_t} / T - \mathbb{E}P_{\hat{R}_t}\|_{op}}{d_{p_0}(\mathbb{E}P_{\hat{R}_t})} \wedge \sqrt{2p_0}, \quad (\text{C.8})$$

so the convergence of $\|P_{\hat{R}} - P_R\|_F$ naturally depends on the expected projection matrix $\mathbb{E}P_{\hat{R}_t}$, the denominator, and on matrix concentration, the numerator.

C.2 Non-degenerated Case

We first show convergence of $\|P_{\widehat{R}} - P_R\|_F$ in the non-degenerated case, where $p_0 = r_0 \leq q_0$. After spherical neighbour arguments, the model is reset as $X_t = RF_tC^\top + E_t$ with E_t left spherical.

C.2.1 Expected Projection Matrix

We first take a look at $\mathbb{E}P_{\widehat{R}_t}$, by lemma 3.2, $\mathbb{E}P_{\widehat{R}_t}$ could be decomposed into two separate parts:

$$\mathbb{E}P_{\widehat{R}_t} = \sum_{i=1}^p \lambda_i u_i u_i^\top = \underbrace{\sum_{i=1}^{r_0} \lambda_i u_i u_i^\top}_S + \underbrace{\sum_{j=r_0+1}^p \lambda_j u_j u_j^\top}_N,$$

where $u_i, i \in \{1, \dots, r_0\}$, generate $\text{Span}(R)$ while $u_j, j \in \{r_0 + 1, \dots, p\}$, generate $\text{Span}(R^\perp)$.

Lemma C.1 (Subspace Variance). For E_t left spherical, let $\{\theta_i\}$ be the principal angles between $\text{Span}(\widehat{R}_t)$ and $\text{Span}(R)$, the following equality holds:

$$\text{tr}(N) = \mathbb{E} \left(\sum_{i=1}^{r_0} \sin^2 \theta_i \right) = \mathbb{E} \|P_{\widehat{R}_t} - P_R\|_F^2 / 2.$$

Proof. Now that $\mathbb{E}P_{\widehat{R}_t}$ and P_R share eigenspace, It is easy to see that:

$$\text{tr}(N) = \text{tr} \left[\mathbb{E}P_{\widehat{R}_t} (I - P_R) \right] = r_0 - \mathbb{E} \text{tr}(P_{\widehat{R}_t} P_R).$$

Since $\text{tr}(P_{\widehat{R}_t} P_R) = \sum_{i=1}^{r_0} \cos^2 \theta_i$ by definition of principal angles, we have acquired the proof. \square

Lemma C.2 (Subspace Deviation). For matrix model $X_t = RF_tC^\top + E_t$, denote σ_{t,r_0} as the r_0 -th singular value of the signal part RF_tC^\top , we have:

$$\|P_{\widehat{R}_t} - P_R\|_F / \sqrt{2} \leq \frac{\sqrt{2r_0} \|E_t\|_{op}}{\sigma_{t,r_0} - \|E_t\|_{op}} \wedge \sqrt{r_0}.$$

Proof. It is a straightforward corollary of Wedin's theorem for perturbation $X_t = RF_tC^\top + E_t$. \square

Since $\text{tr}(\mathbb{E}P_{\widehat{R}_t}) = \mathbb{E} \text{tr}(P_{\widehat{R}_t}) = r_0$, from lemma C.1, C.2 and Assumption A to C, by truncation method as in C.6, we have $\mathbb{E} \|P_{\widehat{R}_t} - P_R\|_F^2 = O(p^{-1/3} + q^{-1/3})$, which means $\text{tr}(S) = \sum_{i=1}^{r_0} \lambda_i \rightarrow r_0$ and $\text{tr}(N) = \sum_{j=r_0+1}^p \lambda_j \rightarrow 0$ as $p, q \rightarrow \infty$. Since $0 \leq \lambda_i \leq 1$ for $i \in \{1, 2, \dots, p\}$, we have $\lambda_{r_0} \rightarrow 1$, $\lambda_{r_0+1} \rightarrow 0$ and naturally $d_{r_0}(\mathbb{E}P_{\widehat{R}_t}) \rightarrow 1$ as $p, q \rightarrow \infty$.

C.2.2 Matrix Concentration

We then turn to the matrix concentration problem on the numerator of C.8. Taking direct advantage of lemma 3.1 would give $\|P_{\widehat{R}} - P_R\|_F = O_p(\sqrt{\log p/T})$. This dimensional factor is inherent in existing matrix concentration results. Alternatively, by triangular inequality and taking expectation on both sides:

$$\mathbb{E} \|P_{\widehat{R}_t} - \mathbb{E}P_{\widehat{R}_t}\|_{op} \leq \mathbb{E} \|P_{\widehat{R}_t} - P_R\|_{op} + \|P_R - \mathbb{E}P_{\widehat{R}_t}\|_{op},$$

where $\|P_R - \mathbb{E}P_{\hat{R}_t}\|_{op} \leq \text{tr}(N) = O(p^{-1/3} + q^{-1/3})$, while $\mathbb{E}\|P_{\hat{R}_t} - P_R\|_{op} \leq \mathbb{E}\|P_{\hat{R}_t} - P_R\|_F = O(p^{-1/4} + q^{-1/4})$ by applying truncation method as in C.6 to lemma C.2. In the end, since $\|P_{\hat{R}_t} - \mathbb{E}P_{\hat{R}_t}\|_{op} \leq 1$ almost surely, by applying Jensen's inequality and scalar concentration to C.8:

$$\|P_{\hat{R}} - P_R\|_F \leq \frac{2\sqrt{2r_0} \sum_{t=1}^T \|P_{\hat{R}_t} - \mathbb{E}P_{\hat{R}_t}\|_{op}}{Td_{r_0}(\mathbb{E}P_{\hat{R}_t})} = O_p(T^{-1/2} + p^{-1/4} + q^{-1/4}),$$

which could be absorbed into the non-spherical deviation term from the previous section.

C.3 Degenerated Case

Then we discuss the degenerated case where $p_0 > q_0 = r_0$. For each data matrix $X_t = RF_tC^\top + E_t$, the signal part RF_tC^\top is at most rank r_0 . It is then natural to set \hat{R}_t to be the leading r_0 left singular vectors of X_t . Then, MPCA_{op} calculates the p_0 leading eigenvectors of average projection matrices $\sum_t P_{\hat{R}_t}/T$, denoted as \hat{R}/\sqrt{p} . As we discussed earlier, the manifold center intuition no longer holds under degeneration. Fortunately, the previous arguments on non-degenerated cases could be transferred readily to degenerated ones with only slight adjustments.

C.3.1 Expected Projection Matrix

By lemma 3.2, $\mathbb{E}P_{\hat{R}_t}$ could still be decomposed into two separate parts:

$$\mathbb{E}P_{\hat{R}_t} = \sum_{i=1}^p \lambda_i u_i u_i^\top = \underbrace{\sum_{i=1}^{p_0} \lambda_i u_i u_i^\top}_S + \underbrace{\sum_{j=p_0+1}^p \lambda_j u_j u_j^\top}_N, \quad (\text{C.9})$$

where $u_i, i \in \{1, \dots, p_0\}$, generate $\text{Span}(R)$ while $u_j, j \in \{p_0 + 1, \dots, p\}$, generate $\text{Span}(R^\perp)$. As in the non-degenerated case, $\text{tr}(S) = \mathbb{E}\text{tr}(P_{\hat{R}_t} P_R)$ and $\text{tr}(N) = r_0 - \mathbb{E}\text{tr}(P_{\hat{R}_t} P_R)$. Take a further look at \hat{R}_t , the leading r_0 left singular vectors of $X_t = RF_tC^\top + E_t$. It is actually the perturbation of R_t , the r_0 left singular vectors of the signal part RF_tC^\top . Actually, $\text{Span}(R_t)$ is a r_0 -dimensional random subspace of $\text{Span}(R)$, the randomness comes from signal F_t . Then P_R could be decomposed into two parts as $P_R = P_{R_t} + P_{R_t^\perp}$, the second term corresponds to the $(p_0 - r_0)$ -dimensional subspace left. We have:

$$\text{tr}(S) = \mathbb{E}\text{tr}(P_{\hat{R}_t} P_{R_t}) + \mathbb{E}\text{tr}(P_{\hat{R}_t} P_{R_t^\perp}) \geq \mathbb{E}\text{tr}(P_{\hat{R}_t} P_{R_t}),$$

where $\mathbb{E}\text{tr}(P_{\hat{R}_t} P_{R_t}) = r_0 - \mathbb{E}\|P_{\hat{R}_t} - P_{R_t}\|_F^2/2$, and $\mathbb{E}\|P_{\hat{R}_t} - P_{R_t}\|_F^2/2$ could be viewed as subspace variance and controlled by arguments as in lemma C.2. Since $\text{tr}(S) \leq \text{tr}(\mathbb{E}P_{\hat{R}_t}) = r_0$, we have $\text{tr}(S) = \sum_{i=1}^{p_0} \lambda_i \rightarrow r_0$ and $\text{tr}(N) = \sum_{j=p_0+1}^p \lambda_j \rightarrow 0$ as $p, q \rightarrow \infty$. The problem is that now $\text{tr}(S) \rightarrow r_0$ is distributed within p_0 eigenvalues, which gives chance for really small eigenvalue λ_{p_0} , while the eigengap $d_{p_0}(\mathbb{E}P_{\hat{R}_t}) = \lambda_{p_0} - \lambda_{p_0+1}$ needs to be positive to ensure convergence. Fortunately, positive eigengap is justified by the following lemma.

Lemma C.3 (Positive Eigengap). Under Assumption A to C, there exists $c > 0$ free of p and q such that the eigengap $d_{p_0}(\mathbb{E}P_{\hat{R}_t}) = \lambda_{p_0} - \lambda_{p_0+1} \geq c$ as $p, q \rightarrow \infty$.

Proof. First we prove there exists $c > 0$ such that $d_{p_0}(\mathbb{E}P_{R_t}) > c$, where R_t would be the r_0 leading left singular vectors of the signal part $RF_tC^\top = \zeta_t R \Sigma_1^{1/2} Z_t^F \Sigma_2^{1/2} C^\top$. By stochastic representation of matrix spherical distributions given in [Gupta and Nagar \(2018\)](#), we could decompose Z_t^F into three independent parts, namely $Z_t^F = U_t D_t V_t^\top$. Here U_t of shape $p_0 \times q_0$ and V_t of shape $q_0 \times q_0$ are uniformly distributed orthonormal matrices, while D_t is diagonal. Clearly, $\text{Span}(R_t) = \text{Span}(R \Sigma_1^{1/2} U_t)$ and:

$$P_{R_t} = (R \Sigma_1^{1/2} U_t) \left(U_t^\top \Sigma_1 U_t \right)^{-1} (U_t^\top \Sigma_1^{1/2} R^\top) / p. \quad (\text{C.10})$$

Here $U_t^\top \Sigma_1 U_t$ is invertible since it is a $q_0 \times q_0$ sub-matrix of a $p_0 \times p_0$ positive definite matrix $\dot{U}_t^\top \Sigma_1 \dot{U}_t$, where \dot{U}_t is acquired by filling U_t to $p_0 \times p_0$ orthonormal. In fact, the smallest eigenvalue of $(U_t^\top \Sigma_1 U_t)^{-1}$ is larger than $1/C_1$ almost surely. Since $\text{Span}(R_t)$ is random subspace of $\text{Span}(R)$, the $(p_0 + 1)$ -th eigenvalue of $\mathbb{E}P_{R_t}$ is clearly 0, we only need to show that $\langle u, \mathbb{E}P_{R_t} u \rangle > c$ for all $u \in \text{Span}(R)$, $\|u\|_2 = 1$. For $u \in \text{Span}(R)$, $\|u\|_2 = 1$, it is not hard to verify that $R^\top u / \sqrt{p}$ would be a unit vector in \mathbb{R}^{p_0} , so that $\|\Sigma_1^{1/2} R^\top u / \sqrt{p}\|_2 \geq \sqrt{c_1}$ under Assumption B. For unit vector $v = (\Sigma_1^{1/2} R^\top u) / \|\Sigma_1^{1/2} R^\top u\|_2$, from C.10 we have $\langle u, \mathbb{E}P_{R_t} u \rangle \geq c_1 \mathbb{E} \langle U_t^\top v, (U_t^\top \Sigma_1 U_t)^{-1} U_t^\top v \rangle$ almost surely, and the right hand side is free of p and q . Now that $\lambda_{q_0}((U_t^\top \Sigma_1 U_t)^{-1}) \geq 1/C_1$ almost surely, if we assume that $\mathbb{E} \langle U_t^\top v, (U_t^\top \Sigma_1 U_t)^{-1} U_t^\top v \rangle = 0$, we should have $U_t^\top v = 0$ almost surely, which leads to contradiction.

In the end since $\|\mathbb{E}P_{\hat{R}_t} - \mathbb{E}P_{R_t}\|_{op} \leq \mathbb{E}\|P_{\hat{R}_t} - P_{R_t}\|_{op}$ by Jensen's inequality, while the latter goes to 0 when $p, q \rightarrow \infty$ as we discussed earlier, apply Weyl's inequality to acquire the proof. \square

C.3.2 Matrix Concentration

We then turn to the matrix concentration problem on the numerator of C.8. Again taking direct advantage of lemma 3.1 would give $\|P_{\hat{R}} - P_R\|_F = O_p(\sqrt{\log p/T})$. Fortunately, in this case of random projection matrices, we are able to shrink the dimensional factor p to r_0 via intrinsic dimension arguments. According to matrix Bernstein inequality in Hermitian case with intrinsic dimension from [Tropp \(2015\)](#), we only need to focus on the independent centered term $\mathcal{P}_t = P_{\hat{R}_t} - \mathbb{E}P_{\hat{R}_t}$. First, $\|\mathcal{P}_t\|_{op} \leq 1$ almost surely. Then, consider the matrix variance $\mathbb{E}\mathcal{P}_t^2 = \mathbb{E}P_{\hat{R}_t}^2 - (\mathbb{E}P_{\hat{R}_t})^2$. Under left spherical E_t , the eigenvalues of $\mathbb{E}\mathcal{P}_t^2$ are precisely $\lambda_i - \lambda_i^2$, $i \in \{1, 2, \dots, p_0\}$, and $\lambda_j - \lambda_j^2 \rightarrow 0$ for $j \in \{p_0 + 1, p_0 + 2, \dots, p\}$, where λ_i and λ_j are eigenvalues of S and N from C.9 respectively. Since there exists $c > 0$ such that $\lambda_{p_0} \geq c$ according to lemma C.3, while $\lambda_{p_0} \leq r_0/p_0$ automatically, there exists $C > 0$ free of p and q such that $C \leq \|\mathbb{E}\mathcal{P}_t^2\|_{op} \leq 1/4$. So the intrinsic dimension of $\mathbb{E}\mathcal{P}_t^2$, namely $\text{intdim}(\mathbb{E}\mathcal{P}_t^2) = \text{tr}(\mathbb{E}\mathcal{P}_t^2) / \|\mathbb{E}\mathcal{P}_t^2\|_{op} \lesssim r_0$ does not grow with matrix dimension, and we could replace p in lemma 3.1 with r_0 as:

$$\mathbb{P} \left\{ \left\| \sum_{t=1}^T (P_{\hat{R}_t} - \mathbb{E}P_{\hat{R}_t}) \right\|_{op} \geq x \right\} \lesssim r_0 \cdot \exp \left\{ \frac{-x^2/2}{T \|\mathbb{E}\mathcal{P}_t^2\|_{op} + x/3} \right\}.$$

By applying dimension-free convergence, $\|P_{\hat{R}} - P_R\|_F = O_p(T^{-1/2})$. In the end, take the deviation from noise being non-spherical into account, we claim the proof.

D Proof of Theorem 3.4

We only discuss $\text{Span}(R)$ here due to symmetry. Recall that for MPCA_F , $\widehat{R}_t^{(i)}$ would be the leading $r_0 = p_0 \wedge q_0$ eigenvalues of $X_t P_{\widehat{C}^{(i-1)}} X_t^\top$ if $\widehat{C}^{(i-1)}$ is given. Let $C^{(i-1)} = \widehat{C}^{(i-1)} / \sqrt{q}$ for notational simplicity. We focus on the projected matrix model $X_t C^{(i-1)} = R F_t C^\top + E_t C^{(i-1)}$, and $\widehat{R}_t^{(i)}$ would exactly be the result of applying MPCA_{op} to the projected data set $\{X_t C^{(i-1)}\}$. It is worth mentioning that multiplying $C^{(i-1)}$ on the right does not effect the left properties we need in section C: for instance, if E_t is left spherical, then $E_t C^{(i-1)}$ is still left spherical, so the proof from section C could adjust to the projected data set readily.

The difference lies in the signal-to-noise ratio. In section C, let σ_{t,r_0} be the r_0 -th singular value of the signal part $S_t = R F_t C^\top$, then $\sigma_{t,r_0} \gtrsim (pq)^{1/2} \zeta_t \sigma_{r_0}(Z_t^F)$ and $\|E_t\|_{op} \lesssim \zeta_t \|Z_t^E\|_{op}$. It is foreseeable that we could increase the signal-to-noise ratio via projection by some $\widehat{C}^{(i-1)}$ sufficiently close to C , keeping the signal size almost unchanged. It is ensured by assuming $\sigma_{q_0}(C^\top \widehat{C}^{(i-1)})/q = c > 0$.

In essence, let $\sigma_{t,r_0}^{(i-1)}$ be the r_0 -th singular value of the projected signal part $S_t C^{(i-1)} = R F_t C^\top C^{(i-1)}$. If $p_0 = r_0 \leq q_0$, consider the matrix $S_t P_{C^{(i-1)}} S_t^\top = R F_t C^\top P_{C^{(i-1)}} C F_t^\top R^\top$, whose r_0 -th eigenvalue is $(\sigma_{t,r_0}^{(i-1)})^2$. Let $v = Ru/\sqrt{p}$, $\|u\|_2 = 1$ be the unit vector of r_0 -dimensional subspace $\text{Span}(R)$, then $\langle v, S_t P_{C^{(i-1)}} S_t^\top v \rangle = p \langle u, F_t C^\top P_{C^{(i-1)}} C F_t^\top u \rangle \geq p \sigma_{r_0}^2(F_t C^\top C^{(i-1)}) \geq pq(c_1 c \zeta_t)^2 \sigma_{r_0}^2(Z_t^F)$, $\forall v \in \text{Span}(R)$, the last inequality comes from $\|\Sigma_1^{1/2} Z_t^F \Sigma_2^{1/2} C^\top C^{(i-1)} w\|_2 \geq q^{1/2} c_1 c \sigma_{r_0}(Z_t^F)$ for all $\|w\|_2 = 1$. In the end, by Courant–Fischer’s minimax theorem, $\sigma_{t,r_0}^{(i-1)} \geq (pq)^{1/2} c_1 c \zeta_t \sigma_{r_0}(Z_t^F)$. If $p_0 > q_0 = r_0$, then similarly, since $\|(C^{(i-1)})^\top C \Sigma_2^{1/2} (Z_t^F)^\top \Sigma_1^{1/2} R^\top w\|_2 \geq (pq)^{1/2} c_1 c \sigma_{r_0}(Z_t^F)$ for all $w \in \text{Span}(R)$ and $\|w\|_2 = 1$, we still have $\sigma_{t,r_0}^{(i-1)} \geq (pq)^{1/2} c_1 c \zeta_t \sigma_{r_0}(Z_t^F)$.

As for the noise part, let $E_t = \zeta_t \Omega_1^{1/2} Z_t^E \Omega_1^{1/2}$ with $\zeta_t = r_t / \|Z_t\|_2$, we need to prove that:

$$\|E_t C^{(i-1)}\|_{op} = \sup_{\|v\|_2=1} \|E_t C^{(i-1)} v\|_2 \lesssim \zeta_t p^{1/2}.$$

First, $u = \Omega_1^{1/2} C^{(i-1)} v$ spans a q_0 -dimensional subspace of the q -dimensional space, with $c_2^{1/2} \leq \|u\|_2 \leq C_2^{1/2}$ under Assumption C. For $E_t C^{(i-1)} v = r_t \Omega_1^{1/2} Z_t^E u / \|Z_t\|_2$, since Z_t^E is rotation invariant while $\|Z_t\|_2$ remains unchanged under rotation as shown in section B, there is no loss of generality if we rotate $\text{Span}(u)$ to be $\text{Span}(e_1, e_2, \dots, e_{q_0})$, where $\{e_1, e_2, \dots, e_{q_0}\}$ are the first q_0 Euclidean basis vectors. It is equivalent to say that only the first q_0 elements in vector u can be non-zero. That is to say, we should only take the first q_0 columns of Z_t^E into account when maximizing $\zeta_t \Omega_1^{1/2} Z_t^E u$, which is a $p \times q_0$ random matrix with i.i.d. standard Gaussian elements, and directly $\|E_t C^{(i-1)}\|_{op} \lesssim \zeta_t p^{1/2}$.

The proof is then identical to section C, since projection effects the signal-to-noise ratio, the convergence rate for $\widehat{R}^{(i)}$ given $\widehat{C}^{(i-1)}$ would be $O_p(T^{-1} + q^{-1/2})$.

E Proof of Corollary 3.1

For $\widehat{F}_t = \widehat{R}^\top X_t \widehat{C} / (pq)$, plug in $X_t = R F_t C^\top + E_t$ and get:

$$\widehat{F}_t = \widehat{R}^\top R F_t C^\top \widehat{C} / (pq) + \widehat{R}^\top E_t \widehat{C} / (pq). \quad (\text{E.1})$$

Recall that $\zeta_t = r_t / \|Z_t\|_2 = O_p(1)$ under Assumption B, let $\varepsilon_R = \widehat{R} - R H_R$ and $\varepsilon_C = \widehat{C} - C H_C$,

for the latter term we have:

$$\begin{aligned}\widehat{R}^\top E_t \widehat{C} &= (RH_R + \varepsilon_R)^\top E_t (CH_C + \varepsilon_C) \\ &= H_R^\top R^\top E_t CH_C + H_R^\top R^\top E_t \varepsilon_C + \varepsilon_R^\top E_t CH_C + \varepsilon_R^\top E_t \varepsilon_C,\end{aligned}\tag{E.2}$$

where $\|H_R^\top R^\top E_t CH_C\|_{op} = O_p((pq)^{1/2})$ by similar projection arguments as in section D, it is consistent with results in Yu et al. (2021). Take $\|\cdot\|_{op}$ on both sides of E.2, since $E_t = O_p((pq)^{1/2})$, $\|\varepsilon_R/\sqrt{p}\|_{op} = o_p(1)$, $\|\varepsilon_C/\sqrt{q}\|_{op} = o_p(1)$, by sub-multiplicativity of operator norm and triangular inequality we have:

$$\|\widehat{R}^\top E_t \widehat{C}\|_{op}/(pq) = O_p\left(\|\frac{\varepsilon_R}{\sqrt{p}}\|_{op} + \|\frac{\varepsilon_C}{\sqrt{q}}\|_{op} + (pq)^{-1/2}\right).\tag{E.3}$$

As for the former term on the right hand side of E.1, we have:

$$\begin{aligned}\widehat{R}^\top R F_t C^\top \widehat{C} &= (RH_R + \varepsilon_R)^\top R F_t C^\top (CH_C + \varepsilon_C) \\ &= pq H_R^\top F_t H_C + p H_R^\top F_t C^\top \varepsilon_C + q \varepsilon_R^\top R F_t H_C + \varepsilon_R^\top R F_t C^\top \varepsilon_C.\end{aligned}\tag{E.4}$$

By arranging E.1, E.3, E.4 and taking $\|\cdot\|_{op}$ on both sides, due to sub-multiplicativity of operator norm and triangular inequality, we have:

$$\|\widehat{F}_t - H_R^\top F_t H_C\|_{op} = O_p\left(\|\frac{\varepsilon_R}{\sqrt{p}}\|_{op} + \|\frac{\varepsilon_C}{\sqrt{q}}\|_{op} + (pq)^{-1/2}\right).$$

Similarly, let $\varepsilon_F = \widehat{F}_t - H_R^\top F_t H_C$, we have:

$$\begin{aligned}\widehat{S}_t - S_t &= \widehat{R} \widehat{F}_t \widehat{C}^\top - R F_t C^\top \\ &= (RH_R + \varepsilon_R)(H_R^\top F_t H_C + \varepsilon_F)(CH_C + \varepsilon_C)^\top - R F_t C^\top \\ &= R F_t H_C \varepsilon_C^\top + R H_R \varepsilon_F H_C^\top C^\top + R H_R \varepsilon_F \varepsilon_C^\top + \varepsilon_R H_R^\top F_t C^\top \\ &\quad + \varepsilon_R H_R^\top F_t H_C \varepsilon_C^\top + \varepsilon_R \varepsilon_F H_C^\top C^\top + \varepsilon_R \varepsilon_F \varepsilon_C^\top.\end{aligned}$$

Again, take $\|\cdot\|_{op}$ on both sides, by sub-multiplicativity of operator norm and triangular inequality:

$$\|\widehat{S}_t - S_t\|_{op}/\sqrt{pq} = O_p\left(\|\frac{\varepsilon_R}{\sqrt{p}}\|_{op} + \|\frac{\varepsilon_C}{\sqrt{q}}\|_{op} + (pq)^{-1/2}\right).$$

F Proof of Theorem 4.2

Here we only prove \widehat{p}_0 due to symmetry. Now that:

$$\mathbb{P}(\widehat{p}_0 = p_0) \geq \mathbb{P}(\widehat{p}_0 = p_0, \widehat{r}_0 = r_0) = \mathbb{P}(\widehat{r}_0 = r_0) \mathbb{P}(\widehat{p}_0 = p_0 \mid \widehat{r}_0 = r_0),$$

it suffices to prove that $\mathbb{P}(\widehat{r}_0 = r_0) \rightarrow 1$ and $\mathbb{P}(\widehat{p}_0 = p_0 \mid \widehat{r}_0 = r_0) \rightarrow 1$. As for the first part, $\mathbb{P}(\widehat{r}_{0,t} = r_0) \rightarrow 1$ under Assumption A to C, since $\widehat{r}_{0,t}$ is determined by each data matrix $X_t = R F_t C^\top + E_t$ and the signal part goes to infinity faster than noise. So directly $\mathbb{P}(\widehat{r}_0 = r_0) \rightarrow 1$.

As for the second part, under condition $\widehat{r}_0 = r_0$, meaning that true compression rank r_0 is acquired, \widehat{R}_t would be exactly \widehat{R}_t in MPCA_{op}. Under spherical neighbour arguments in section C, apply

Jensen's inequality to C.7 to get $\|\sum_{t=1}^T (P_{\hat{R}_t} - \dot{P}_{\hat{R}_t})/T\|_{op} = o_p(1)$, to C.5 to get $\|\mathbb{E}P_{\hat{R}_t} - \mathbb{E}\dot{P}_{\hat{R}_t}\|_{op} = o(1)$. Then, take $\|\sum_{t=1}^T \dot{P}_{\hat{R}_t}/T - \mathbb{E}\dot{P}_{\hat{R}_t}\|_{op} = o_p(1)$ from section C, by triangular inequality we have $\|\sum_{t=1}^T P_{\hat{R}_t}/T - \mathbb{E}P_{\hat{R}_t}\|_{op} = o_p(1)$ as $T, p, q \rightarrow \infty$. In addition, now that $\lambda_{p_0}(\mathbb{E}\dot{P}_{\hat{R}_t}) \geq c > 0$ while $\lambda_{p_0+1}(\mathbb{E}\dot{P}_{\hat{R}_t}) \rightarrow 0$ as $p, q \rightarrow \infty$, by Weyl's inequality, $\|\mathbb{E}P_{\hat{R}_t} - \mathbb{E}\dot{P}_{\hat{R}_t}\|_{op} = o(1)$ and $\|\sum_{t=1}^T P_{\hat{R}_t}/T - \mathbb{E}P_{\hat{R}_t}\|_{op} = o_p(1)$ we have $\mathbb{P}(\hat{p}_0 = p_0 \mid \hat{r}_0 = r_0) \rightarrow 1$.

G Additional Simulation Results

Table 6: Means and standard deviations (in parentheses) of $\mathcal{D}(\widehat{R}, R)$ and $\mathcal{D}(\widehat{C}, C)$ over 100 replications with $s_E = 1.5$ and $T = 3(pq)^{1/2}$. Here MPCA_{op} and MPCA_F stands for Manifold PCA methods; $(2D)^2$ -PCA is from [Zhang and Zhou \(2005\)](#), it is equivalent to α -PCA by [Chen and Fan \(2021\)](#) with $\alpha = -1$; PE stands for the projected estimation by [Yu et al. \(2021\)](#).

Distribution	Evaluation	p	q	MPCA_{op}	MPCA_F	$(2D)^2$ -PCA	PE
Gaussian	$\mathcal{D}(\widehat{R}, R)$	20	20	(0.4859,0.0885)	(0.1702,0.0412)	(0.4314,0.1167)	(0.1372,0.0377)
		20	100	(0.5261,0.0579)	(0.0535,0.0082)	(0.4293,0.1207)	(0.0361,0.0064)
		100	100	(0.2646,0.0994)	(0.0591,0.0040)	(0.2982,0.1353)	(0.0514,0.0040)
	$\mathcal{D}(\widehat{C}, C)$	20	20	(0.4898,0.0952)	(0.1756,0.0468)	(0.4410,0.1271)	(0.1419,0.0521)
		20	100	(0.1026,0.0115)	(0.0910,0.0082)	(0.0863,0.0113)	(0.0784,0.0089)
		100	100	(0.2625,0.0886)	(0.0586,0.0039)	(0.2932,0.1267)	(0.0509,0.0039)
t_3	$\mathcal{D}(\widehat{R}, R)$	20	20	(0.6169,0.0693)	(0.3567,0.1261)	(0.6974,0.0892)	(0.5756,0.1938)
		20	100	(0.5560,0.0391)	(0.0829,0.0135)	(0.6107,0.0748)	(0.2065,0.2175)
		100	100	(0.6091,0.0222)	(0.0968,0.0077)	(0.7433,0.1208)	(0.4291,0.3020)
	$\mathcal{D}(\widehat{C}, C)$	20	20	(0.6232,0.0649)	(0.3723,0.1308)	(0.6880,0.0866)	(0.5782,0.2010)
		20	100	(0.2285,0.0479)	(0.1454,0.0165)	(0.3655,0.1833)	(0.2800,0.2107)
		100	100	(0.6092,0.0277)	(0.0977,0.0072)	(0.7398,0.1204)	(0.4247,0.3019)
t_1	$\mathcal{D}(\widehat{R}, R)$	20	20	(0.0700,0.0177)	(0.0522,0.0076)	(0.8259,0.1215)	(0.8402,0.1488)
		20	100	(0.0415,0.0096)	(0.0231,0.0030)	(0.8677,0.0953)	(0.8793,0.1189)
		100	100	(0.0147,0.0010)	(0.0149,0.0009)	(0.9769,0.0240)	(0.9807,0.0253)
	$\mathcal{D}(\widehat{C}, C)$	20	20	(0.0689,0.0145)	(0.0507,0.0075)	(0.8304,0.1164)	(0.8432,0.1339)
		20	100	(0.0296,0.0027)	(0.0316,0.0025)	(0.9519,0.0850)	(0.9578,0.1005)
		100	100	(0.0147,0.0011)	(0.0151,0.0009)	(0.9762,0.0292)	(0.9831,0.0198)
α -stable	$\mathcal{D}(\widehat{R}, R)$	20	20	(0.6460,0.0612)	(0.4506,0.1279)	(0.8692,0.0598)	(0.8834,0.0781)
		20	100	(0.5714,0.0449)	(0.0988,0.0171)	(0.8873,0.0437)	(0.9080,0.0454)
		100	100	(0.9013,0.0449)	(0.1188,0.0091)	(0.9846,0.0071)	(0.9854,0.0070)
	$\mathcal{D}(\widehat{C}, C)$	20	20	(0.6502,0.0592)	(0.4507,0.1374)	(0.8713,0.0613)	(0.8887,0.0740)
		20	100	(0.3284,0.0861)	(0.1654,0.0174)	(0.9606,0.0400)	(0.9787,0.0287)
		100	100	(0.9022,0.0543)	(0.1188,0.0087)	(0.9834,0.0074)	(0.9843,0.0069)
skewed- t_3	$\mathcal{D}(\widehat{R}, R)$	20	20	(0.6189,0.0643)	(0.3869,0.1410)	(0.7403,0.0909)	(0.6967,0.1768)
		20	100	(0.5480,0.0465)	(0.0813,0.0150)	(0.6245,0.0882)	(0.2654,0.2657)
		100	100	(0.6299,0.0296)	(0.0951,0.0066)	(0.8033,0.1176)	(0.5844,0.3226)
	$\mathcal{D}(\widehat{C}, C)$	20	20	(0.6070,0.0768)	(0.3616,0.1408)	(0.7421,0.0955)	(0.6961,0.1930)
		20	100	(0.2161,0.0469)	(0.1375,0.0150)	(0.4176,0.2039)	(0.3341,0.2542)
		100	100	(0.6265,0.0239)	(0.0945,0.0068)	(0.8072,0.1158)	(0.5877,0.3136)

Table 7: Means and standard deviations (in parentheses) of $\mathcal{D}(\widehat{R}, R)$ and $\mathcal{D}(\widehat{C}, C)$ over 100 replications with $s_E = 2$ and $T = 3(pq)^{1/2}$. Here MPCA_{op} and MPCA_F stands for Manifold PCA methods; $(2D)^2$ -PCA is from [Zhang and Zhou \(2005\)](#), it is equivalent to α -PCA by [Chen and Fan \(2021\)](#) with $\alpha = -1$; PE stands for the projected estimation by [Yu et al. \(2021\)](#).

Distribution	Evaluation	p	q	MPCA_{op}	MPCA_F	$(2D)^2$ -PCA	PE
Gaussian	$\mathcal{D}(\widehat{R}, R)$	20	20	(0.5463,0.0752)	(0.2518,0.0795)	(0.5284,0.0818)	(0.2209,0.0882)
		20	100	(0.5409,0.0430)	(0.0660,0.0110)	(0.5195,0.0635)	(0.0484,0.0096)
		100	100	(0.5380,0.0466)	(0.0755,0.0052)	(0.5580,0.0304)	(0.0687,0.0049)
	$\mathcal{D}(\widehat{C}, C)$	20	20	(0.5648,0.0592)	(0.2668,0.0984)	(0.5447,0.0670)	(0.2315,0.0953)
		20	100	(0.1422,0.0212)	(0.1163,0.0125)	(0.1261,0.0215)	(0.1048,0.0129)
		100	100	(0.5393,0.0460)	(0.0762,0.0052)	(0.5585,0.0273)	(0.0692,0.0051)
t_3	$\mathcal{D}(\widehat{R}, R)$	20	20	(0.7081,0.0763)	(0.5596,0.1189)	(0.7817,0.0755)	(0.7694,0.1298)
		20	100	(0.5696,0.0457)	(0.1143,0.0248)	(0.6824,0.0920)	(0.3751,0.2600)
		100	100	(0.7410,0.0510)	(0.1294,0.0104)	(0.8591,0.1006)	(0.7143,0.2917)
	$\mathcal{D}(\widehat{C}, C)$	20	20	(0.7051,0.0693)	(0.5471,0.1226)	(0.7738,0.0829)	(0.7675,0.1385)
		20	100	(0.4192,0.1217)	(0.1890,0.0203)	(0.6013,0.1564)	(0.4481,0.2478)
		100	100	(0.7408,0.0522)	(0.1296,0.0086)	(0.8587,0.0990)	(0.7108,0.2969)
t_1	$\mathcal{D}(\widehat{R}, R)$	20	20	(0.0821,0.0237)	(0.0594,0.0095)	(0.8699,0.0809)	(0.8957,0.0811)
		20	100	(0.0569,0.0135)	(0.0267,0.0033)	(0.9039,0.0399)	(0.9091,0.0428)
		100	100	(0.0179,0.0014)	(0.0170,0.0009)	(0.9842,0.0067)	(0.9855,0.0062)
	$\mathcal{D}(\widehat{C}, C)$	20	20	(0.0849,0.0193)	(0.0592,0.0090)	(0.8706,0.0672)	(0.8975,0.0703)
		20	100	(0.0361,0.0037)	(0.0364,0.0025)	(0.9798,0.0218)	(0.9834,0.0177)
		100	100	(0.0176,0.0013)	(0.0169,0.0010)	(0.9840,0.0068)	(0.9851,0.0064)
α -stable	$\mathcal{D}(\widehat{R}, R)$	20	20	(0.7404,0.0672)	(0.6178,0.1109)	(0.8953,0.0390)	(0.9104,0.0408)
		20	100	(0.6226,0.0442)	(0.1385,0.0335)	(0.9046,0.0370)	(0.9174,0.0360)
		100	100	(0.9700,0.0157)	(0.2533,0.2459)	(0.9836,0.0081)	(0.9843,0.0076)
	$\mathcal{D}(\widehat{C}, C)$	20	20	(0.7507,0.0702)	(0.6170,0.1215)	(0.8959,0.0456)	(0.9115,0.0376)
		20	100	(0.5948,0.1134)	(0.2171,0.0262)	(0.9774,0.0156)	(0.9842,0.0063)
		100	100	(0.9681,0.0177)	(0.2295,0.2022)	(0.9839,0.0075)	(0.9846,0.0073)
skewed- t_3	$\mathcal{D}(\widehat{R}, R)$	20	20	(0.6981,0.0697)	(0.5468,0.1087)	(0.8213,0.0619)	(0.8328,0.1005)
		20	100	(0.5842,0.0532)	(0.1137,0.0260)	(0.7048,0.0897)	(0.4515,0.2845)
		100	100	(0.8091,0.0651)	(0.1281,0.0103)	(0.9191,0.0655)	(0.8814,0.1871)
	$\mathcal{D}(\widehat{C}, C)$	20	20	(0.7142,0.0755)	(0.5531,0.1118)	(0.8218,0.0735)	(0.8444,0.0990)
		20	100	(0.4068,0.1141)	(0.1905,0.0268)	(0.6639,0.1673)	(0.5606,0.2803)
		100	100	(0.8226,0.0577)	(0.1269,0.0090)	(0.9247,0.0666)	(0.9092,0.1498)

Table 8: Means and standard deviations (in parentheses) of MSE and opMax over 100 replications with $s_E = 1.5$ and $T = 3(pq)^{1/2}$. Here $MPCA_{op}$ and $MPCA_F$ stands for Manifold PCA methods; $(2D)^2$ -PCA is from [Zhang and Zhou \(2005\)](#), it is equivalent to α -PCA by [Chen and Fan \(2021\)](#) with $\alpha = -1$; PE stands for the projected estimation by [Yu et al. \(2021\)](#).

MSE						
Distribution	p	q	$MPCA_{op}$	$MPCA_F$	$(2D)^2$ -PCA	PE
Gauss	20	20	(0.1961,0.0260)	(0.0758,0.0081)	(0.1670,0.0296)	(0.0683,0.0083)
	20	100	(0.0387,0.0108)	(0.0066,0.0003)	(0.0266,0.0075)	(0.0059,0.0003)
	100	100	(0.0134,0.0047)	(0.0027,0.0001)	(0.0161,0.0078)	(0.0025,0.0001)
t_3	20	20	(0.4953,0.0590)	(0.2977,0.0688)	(0.7513,0.3589)	(0.6813,0.4534)
	20	100	(0.0628,0.0082)	(0.0193,0.0013)	(0.1273,0.1098)	(0.0806,0.1168)
	100	100	(0.0575,0.0036)	(0.0079,0.0003)	(0.1415,0.1468)	(0.1068,0.1579)
t_1	20	20	(6.3133,36.191)	(4.5986,23.124)	(2492.6,23518)	(2492.7,23518)
	20	100	(19.744,156.67)	(16.525,126.47)	(5107.7,43364)	(5107.7,43364)
	100	100	(0.4771,2.9825)	(0.4477,2.7605)	(1490.0,7599.4)	(1490.0,7599.4)
α -stable	20	20	(3.4060,16.984)	(3.1931,18.262)	(35.941,250.45)	(36.095,250.43)
	20	100	(0.1256,0.0996)	(0.0515,0.0413)	(5.3870,18.945)	(5.4352,18.946)
	100	100	(0.2104,0.2435)	(0.0476,0.1373)	(18.161,60.959)	(18.173,60.958)
skewed- t_3	20	20	(0.4887,0.0708)	(0.3088,0.0789)	(1.0816,0.8631)	(1.0927,0.9170)
	20	100	(0.0622,0.0087)	(0.0187,0.0013)	(0.1576,0.1347)	(0.1165,0.1595)
	100	100	(0.0609,0.0043)	(0.0078,0.0003)	(0.2176,0.5886)	(0.1974,0.5937)
opMax						
Distribution	p	q	$MPCA_{op}$	$MPCA_F$	$(2D)^2$ -PCA	PE
Gauss	20	20	(0.1264,0.0170)	(0.0758,0.0065)	(0.1133,0.0159)	(0.0757,0.0073)
	20	100	(0.0545,0.0110)	(0.0155,0.0012)	(0.0433,0.0091)	(0.0153,0.0012)
	100	100	(0.0187,0.0047)	(0.0071,0.0004)	(0.0207,0.0066)	(0.0071,0.0005)
t_3	20	20	(0.2551,0.1117)	(0.2119,0.0883)	(0.6100,0.4355)	(0.6526,0.4516)
	20	100	(0.0598,0.0099)	(0.0370,0.0136)	(0.2376,0.2590)	(0.1992,0.2808)
	100	100	(0.0385,0.0070)	(0.0160,0.0057)	(0.3002,0.2869)	(0.2864,0.3061)
t_1	20	20	(1.7080,3.8917)	(1.5531,3.2567)	(17.793,84.060)	(17.794,84.060)
	20	100	(1.6269,7.4722)	(1.5267,6.8267)	(25.729,120.29)	(25.729,120.29)
	100	100	(0.3822,1.1203)	(0.3740,1.0838)	(19.831,63.344)	(19.832,63.344)
α -stable	20	20	(1.1161,2.5846)	(0.9556,2.6376)	(3.9438,9.1424)	(3.9717,9.1340)
	20	100	(0.2179,0.2049)	(0.1697,0.1533)	(2.3220,2.6888)	(2.3308,2.6843)
	100	100	(0.3336,0.3474)	(0.1577,0.2429)	(4.4859,5.0260)	(4.4867,5.0255)
skewed- t_3	20	20	(0.2826,0.1318)	(0.2507,0.1286)	(0.9194,0.6804)	(0.9961,0.6567)
	20	100	(0.0649,0.0163)	(0.0399,0.0143)	(0.2827,0.2790)	(0.2557,0.3077)
	100	100	(0.0401,0.0150)	(0.0179,0.0066)	(0.3965,0.4447)	(0.3925,0.4546)

Table 9: Means and standard deviations (in parentheses) of MSE and opMax over 100 replications with $s_E = 2$ and $T = 3(pq)^{1/2}$. Here $MPCA_{op}$ and $MPCA_F$ stands for Manifold PCA methods; $(2D)^2$ -PCA is from [Zhang and Zhou \(2005\)](#), it is equivalent to α -PCA by [Chen and Fan \(2021\)](#) with $\alpha = -1$; PE stands for the projected estimation by [Yu et al. \(2021\)](#).

MSE						
Distribution	p	q	$MPCA_{op}$	$MPCA_F$	$(2D)^2$ -PCA	PE
Gauss	20	20	(0.3133,0.0297)	(0.1549,0.0276)	(0.2971,0.0298)	(0.1432,0.0303)
	20	100	(0.0485,0.0106)	(0.0116,0.0006)	(0.0443,0.0090)	(0.0107,0.0006)
	100	100	(0.0439,0.0044)	(0.0047,0.0001)	(0.0460,0.0047)	(0.0045,0.0001)
t_3	20	20	(0.8438,0.1168)	(0.6879,0.1074)	(1.4007,0.7806)	(1.4703,0.8140)
	20	100	(0.1073,0.0162)	(0.0360,0.0036)	(0.3363,0.4292)	(0.2782,0.4445)
	100	100	(0.0882,0.0048)	(0.0144,0.0005)	(0.2006,0.1075)	(0.1919,0.1296)
t_1	20	20	(12.0691,70.742)	(10.7265,63.910)	(651.55,4839.8)	(651.66,4839.9)
	20	100	(184.19,1275.9)	(155.09,1063.5)	(80440,663049)	(80440,663049)
	100	100	(0.6902,2.9519)	(0.6519,2.7665)	(1434.6,9685.8)	(1434.6,9685.8)
α -stable	20	20	(4.1815,15.561)	(3.1335,12.560)	(32.625,162.79)	(32.842,162.80)
	20	100	(0.4038,0.8881)	(0.1229,0.2451)	(13.323,69.263)	(13.383,69.264)
	100	100	(1.6554,8.3149)	(0.0981,0.1326)	(37.704,149.03)	(37.749,149.03)
skewed- t_3	20	20	(0.8543,0.2492)	(0.6999,0.2006)	(1.8161,1.3214)	(1.9703,1.3354)
	20	100	(0.1038,0.0125)	(0.0353,0.0029)	(0.3024,0.2596)	(0.2616,0.2885)
	100	100	(0.0986,0.0071)	(0.0143,0.0006)	(0.2907,0.2318)	(0.3079,0.2351)
opMax						
Distribution	p	q	$MPCA_{op}$	$MPCA_F$	$(2D)^2$ -PCA	PE
Gauss	20	20	(0.1536,0.0146)	(0.1104,0.0130)	(0.1506,0.0142)	(0.1110,0.0148)
	20	100	(0.0594,0.0109)	(0.0207,0.0015)	(0.0566,0.0098)	(0.0205,0.0015)
	100	100	(0.0348,0.0039)	(0.0095,0.0006)	(0.0359,0.0040)	(0.0095,0.0006)
t_3	20	20	(0.3410,0.1820)	(0.3184,0.1199)	(0.9777,0.6471)	(1.0549,0.6193)
	20	100	(0.0804,0.0445)	(0.0542,0.0298)	(0.4899,0.5037)	(0.4745,0.5275)
	100	100	(0.0442,0.0147)	(0.0217,0.0060)	(0.4244,0.2420)	(0.4308,0.2528)
t_1	20	20	(2.2703,5.4880)	(2.1404,5.1760)	(15.821,40.776)	(15.824,40.775)
	20	100	(4.6084,22.901)	(4.2820,21.001)	(85.414,480.86)	(85.415,480.86)
	100	100	(0.5571,1.3087)	(0.5456,1.2697)	(20.645,61.759)	(20.645,61.759)
α -stable	20	20	(1.5571,2.5314)	(1.2625,2.1515)	(4.8993,7.9365)	(4.9220,7.9273)
	20	100	(0.4417,0.6399)	(0.2548,0.3278)	(3.2412,4.8479)	(3.2514,4.8433)
	100	100	(0.7617,1.9625)	(0.2440,0.2686)	(6.2133,7.8045)	(6.2145,7.8038)
skewed- t_3	20	20	(0.3958,0.2649)	(0.3815,0.2394)	(1.2478,0.7846)	(1.3338,0.7403)
	20	100	(0.0781,0.0280)	(0.0557,0.0208)	(0.4686,0.3850)	(0.4641,0.4085)
	100	100	(0.0536,0.0238)	(0.0262,0.0120)	(0.5649,0.3378)	(0.5866,0.3244)

Table 10: Frequencies of exact estimation and underestimation (in parentheses) of factor numbers over 100 replications with $s_E = 1.5$ and $T = 3(pq)^{1/2}$. Here MER_{op} and MER_F stands for Manifold eigenvalue-ratio methods; $(2D)^2$ -ER is equivalent to the ER method in [Chen and Fan \(2021\)](#) with $\alpha = -1$; IterER is from [Yu et al. \(2021\)](#).

Distribution	p	q	MER_{op}	MER_F	$(2D)^2$ -ER	IterER
Gaussian	20	20	(0.09,0.39)	(0.77,0.22)	(0.05,0.76)	(0.68,0.32)
	20	100	(0.29,0.06)	(1.00,0.00)	(0.07,0.28)	(1.00,0.00)
	100	100	(0.70,0.00)	(1.00,0.00)	(0.00,0.00)	(1.00,0.00)
t_3	20	20	(0.00,0.97)	(0.12,0.87)	(0.00,0.99)	(0.05,0.94)
	20	100	(0.15,0.75)	(1.00,0.00)	(0.03,0.95)	(0.70,0.11)
	100	100	(0.00,0.98)	(0.87,0.13)	(0.02,0.98)	(0.66,0.33)
t_1	20	20	(0.95,0.05)	(1.00,0.00)	(0.09,0.79)	(0.04,0.75)
	20	100	(0.98,0.02)	(1.00,0.00)	(0.08,0.82)	(0.07,0.80)
	100	100	(1.00,0.00)	(1.00,0.00)	(0.09,0.73)	(0.10,0.76)
α -stable	20	20	(0.01,0.97)	(0.04,0.95)	(0.03,0.97)	(0.04,0.96)
	20	100	(0.01,0.99)	(0.91,0.09)	(0.09,0.88)	(0.05,0.91)
	100	100	(0.00,1.00)	(0.34,0.66)	(0.09,0.81)	(0.02,0.94)
skewed- t_3	20	20	(0.00,0.99)	(0.11,0.88)	(0.00,0.99)	(0.05,0.94)
	20	100	(0.18,0.71)	(0.98,0.02)	(0.06,0.92)	(0.66,0.19)
	100	100	(0.00,1.00)	(0.87,0.13)	(0.02,0.98)	(0.41,0.58)

Table 11: Frequencies of exact estimation and underestimation (in parentheses) of factor numbers over 100 replications with $s_E = 2$ and $T = 3(pq)^{1/2}$. Here MER_{op} and MER_F stands for Manifold eigenvalue-ratio methods; $(2D)^2$ -ER is equivalent to the ER method in [Chen and Fan \(2021\)](#) with $\alpha = -1$; IterER is from [Yu et al. \(2021\)](#).

Distribution	p	q	MER_{op}	MER_F	$(2D)^2$ -ER	IterER
Gaussian	20	20	(0.08,0.72)	(0.39,0.59)	(0.08,0.78)	(0.34,0.62)
	20	100	(0.12,0.10)	(1.00,0.00)	(0.15,0.40)	(0.99,0.01)
	100	100	(0.00,0.00)	(1.00,0.00)	(0.00,0.02)	(1.00,0.00)
t_3	20	20	(0.00,1.00)	(0.00,1.00)	(0.00,1.00)	(0.00,1.00)
	20	100	(0.00,1.00)	(0.93,0.07)	(0.00,1.00)	(0.48,0.44)
	100	100	(0.00,1.00)	(0.25,0.75)	(0.03,0.96)	(0.14,0.86)
t_1	20	20	(0.88,0.12)	(1.00,0.00)	(0.01,0.91)	(0.02,0.88)
	20	100	(0.98,0.02)	(1.00,0.00)	(0.10,0.77)	(0.08,0.79)
	100	100	(1.00,0.00)	(1.00,0.00)	(0.11,0.77)	(0.07,0.80)
α -stable	20	20	(0.00,1.00)	(0.00,1.00)	(0.04,0.95)	(0.05,0.94)
	20	100	(0.00,1.00)	(0.50,0.50)	(0.01,0.95)	(0.01,0.95)
	100	100	(0.00,1.00)	(0.02,0.98)	(0.03,0.85)	(0.02,0.90)
skewed- t_3	20	20	(0.00,1.00)	(0.00,1.00)	(0.00,1.00)	(0.00,1.00)
	20	100	(0.00,1.00)	(0.89,0.11)	(0.00,1.00)	(0.42,0.50)
	100	100	(0.00,1.00)	(0.18,0.82)	(0.03,0.93)	(0.04,0.96)